Supporting information to

# Guest-Triggered $Zn^{II}$ Translocation and Supramolecular Nuclearity Control in Calix[6]arene-Based Complexes

*Nicolas Bernier, Nicolas Menard, Benoit Colasson, Jean-Noël Rebilly* and Olivia Reinaud**

**Experimental section**



**Materials and methods.** Solvents and chemicals were of reagent grade and were used without purification. Calixarene **1** was synthesized according to a published procedure.[1] HR-MS were performed at the Institut de Chimie des Substances Naturelles, Gif-sur-Yvette, France. ESI-MS analyses were obtained with a ThermoFinnigen LCQ Advantage spectrometer using methanol and dichloromethane as solvents. NMR spectra were recorded on a Brucker ARX250 MHz spectrometer or an Advance 500 spectrometer. Illustrations presented throughout the article were obtained using Hyperchem 6.03 for Windows.

**Experimental section**

***1) Synthesis of $L^{TNpy}$***

To a a mixture of calixarene **1** (90 mg, 72 μmol), N-methyl-N-(2-pyridylmethyl)-propargylamine (38 mg, 237 μmol), sodium ascorbate (114 mg, 575 μmol) and $CuSO_4.5H_2O$ (72.5 mg, 287 μmol) were added 0.75 mL of $H_2O$ and 0.75 mL of $CH_2Cl_2$.under argon. The reaction mixture was stirred at room temperature for 15 hours. The residue was diluted with $CH_2Cl_2$ (20 mL) and water (5 mL). ethylenediamine tetraacetic acid bis sodium salt (106 mg, 287 μmol) was added along with 10 drops of aqueous NaOH 3M. The solution was stirred in air for 30 minutes.The organic layer was separated. The aqueous phase extracted with $CH_2Cl_2$ (2x10 mL). The organic extracts were combined and washed with water (10 mL), dried over $Na_2SO_4$, filtered and concentrated. The brown solid was purified by chromatography (basic alumina. Eluent $CH_2Cl_2$ then $CH_2Cl_2$/MeOH 98:2) yielding a pale solid (95 mg, 88%).
**$^1$H (500 MHz, $CD_3CN$, 340 K)** δ (ppm): 1.06 (s, 27H, *t*Bu), 3.08 (s, 9H, OMe), 3.33 (s, 9H, $NMe_{Im}$), 3.70 (m, 12H, $CH_2$py + $CH_2$Tria), 3.81 (s, 12H, $CH_2$Ar), 4.74 (s, 6H, $CH_2$Im), 6.82 (m, 6H, $H_{Im}$), 7.02 (s, 6H, $H_{ArtBu}$), 7.16 (m, 3H, Hpy(meta)), 7.46 (s, 9H, $H_{ArTria}$ + Hpy(meta')), 7.66 (m, 3H, Hpy(para)), 7.84 (m, 3H, $H_{Tria}$), 8.48 (m, 3H, Hpy(ortho)). **$^{13}$C (125 MHz, $CD_3CN$, 300 K)** δ (ppm): 32.13 (*t*Bu + ArCH2), 33.50 (tBu), 35.31 ($NMe_{Im}$), 43.12 ($NMe_{large\ rim}$), 53.46 ($CH_{2Tria}$), 61.64 (OMe), 64.31 ($CH_{2py}$), 68.14 ($CH_{2Im}$), 122.76, 122.93, 123.11, 123.76, 124.22, 127.21, 128.66, 134.23, 134.67, 137.41, 137.49, 145.44, 146.88, 148.19, 150.16, 154.11, 157.89, 161.00. **ESI-MS** ($CH_3OH$) *m/z*: 1755.6 (calc. 1755.9 for $[L^{TNpy}+Na]^+$). **HR-MS** the main peak id associated to mass1733.9702 corresponds to the formula $C_{102}H_{119}N_{21}O_6$ in agreement with $[L^{TNpy} + 2H]^{2+}$ (mass error: 2.9 ppm).

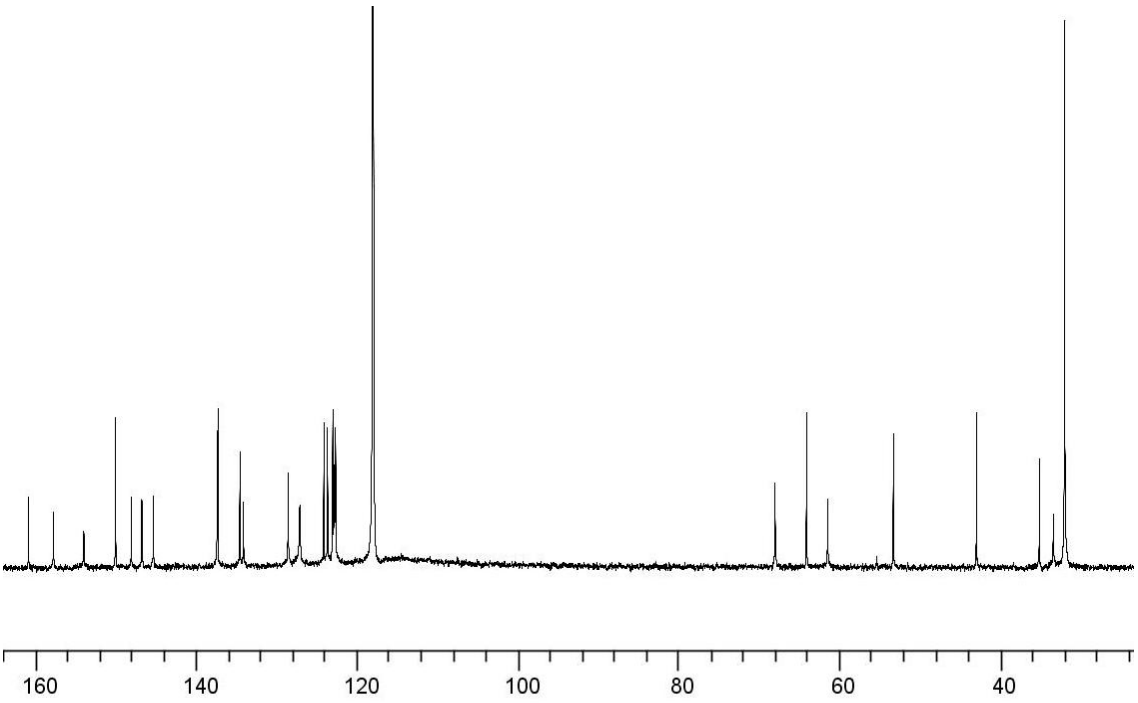


Figure S1. $^{13}$C NMR spectrum of $L^{TNpy}$ (125 MHz, $CD_3CN$, 340K)

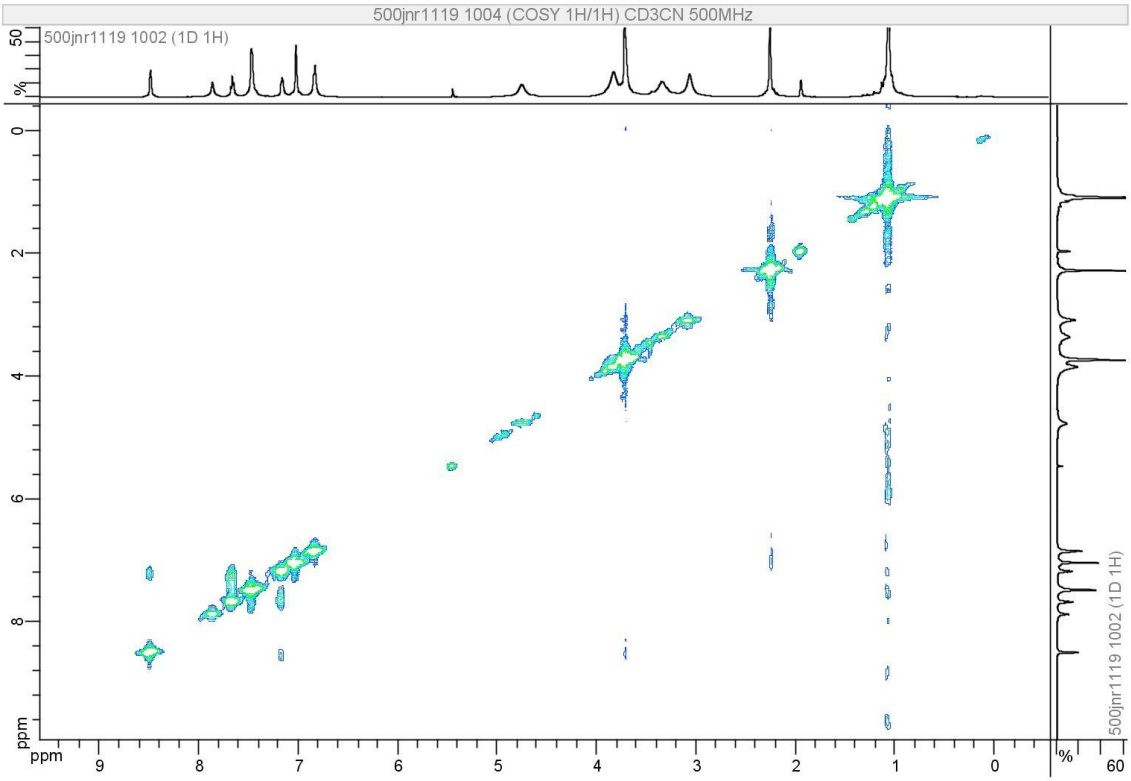


Figure S2. COSY spectrum of $L^{TNpy}$ (500 MHz, $CD_3CN$, 340K)

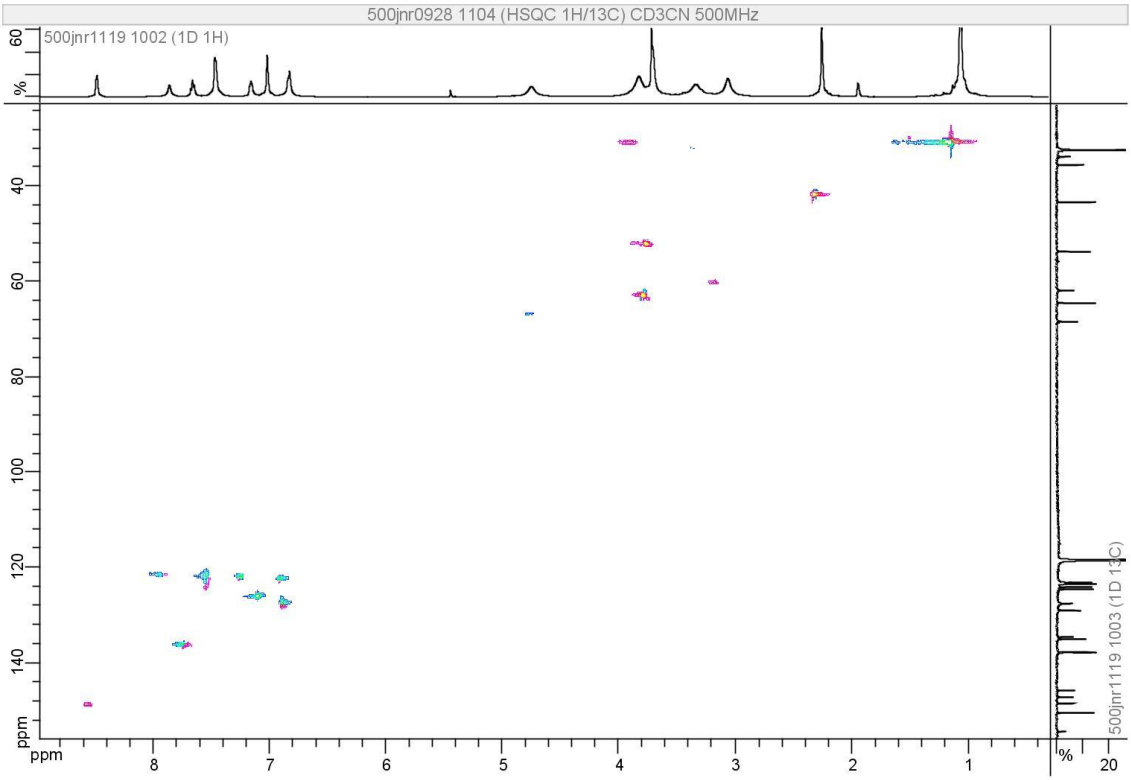


Figure S3. HSQC spectrum of $L^{TNpy}$ (500 MHz, $CD_3CN$, 340K)

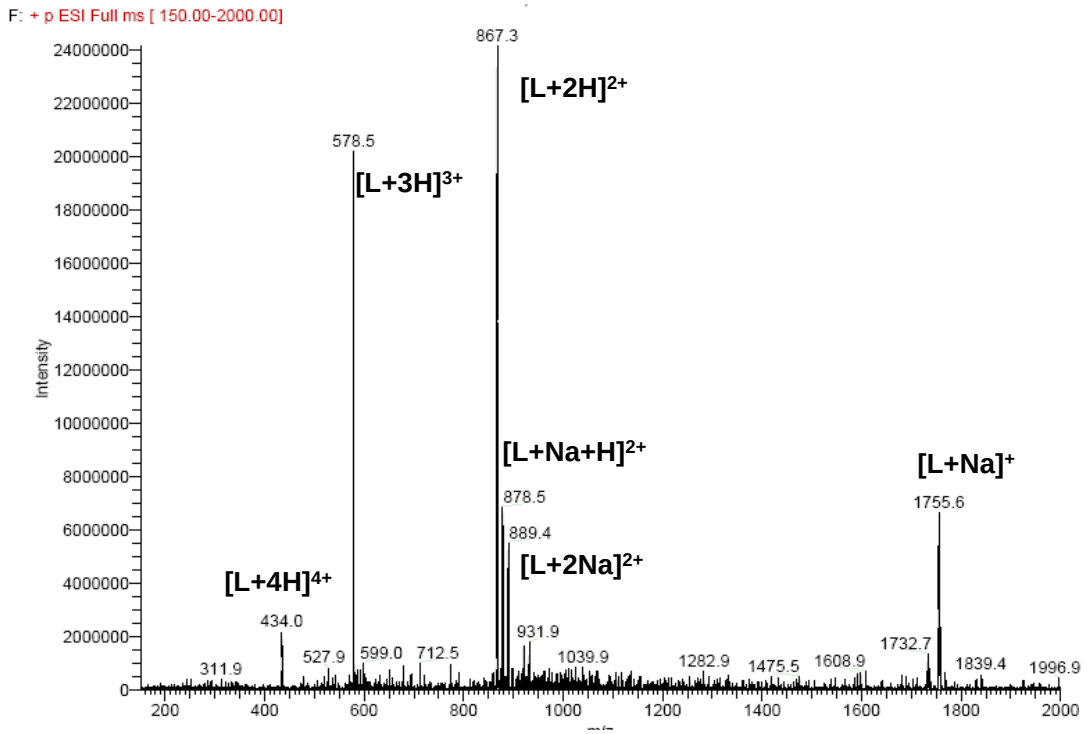


Figure S4. ESI-MS (MeOH) spectrum of $L^{TNpy}$.

## ***2) Synthesis of*** $L^{TNpy}_{C4NHBoc}$

2-a) Synthesis of Zn(**2**)$(ClO_4)_2$

Complex Zn(**1**)$(H_2O)(ClO_4)_2$ (90 mg, 58 μmol), 1-hexynamine (17 mg, 176 μmol) were mixed in 10 mL of toluene and refluxed for three hours. Solvent was evaporated and the residue was washed with diethyl ether (2x10 mL) and dried, yielding a pale solid (84 mg, 89%).

**$^1$H (500 MHz, $CD_3CN$, 300 K)** δ (ppm): -1.09 (m, 2H, β), -0.25 (m, 2H, γ), 0.78 (m, 2H, α), 1.34 (s, 18H, $^t$Bu), 1.41 (s, 9H, $^t$Bu), 1.57 (t, 7.5Hz, 2H, δ), 2.20 (m, 2H, $NH_2$), 3.48 (d, *J* = 14 Hz, 2H, $ArCH_2$), 3.53 (d, *J* = 14 Hz, 2H, $ArCH_2$), 3.57 (s, 6H, $OCH_3$), 3.69 (d, *J* = 14 Hz, 2H, $ArCH_2$), 3.76 (s, 3H, $OCH_3$), 3.77 (s, 6H, $NCH_3$), 3.81 (s, 3H, $NCH_3$), 4.10 (br m, 6H, $ArCH_2$), 5.18 (d, *J* =14.8 Hz, 2H, $ImCH_2$), 5.28 (d, *J* = 14.8 Hz, 2H, $ImCH_2$), 5.38 (s, 2H, $ImCH_2$), 6.10 (s, 2H, $HArN_3$), 6.24 (s, 2H, $HArN_3$), 6.28 (s, 2H, $HAr_{tria}$), 6.87 (s, 1H, ImH),

6.90 (s, 2H, ImH), 7.24 (s, 1H, $H_{tria}$). **$^{13}$C (125 MHz, $CD_3CN$, 300 K)** δ (ppm): 21.9 (δ), 25.2 (γ), 30.7 ($ArCH_2$), 31.3 (β), 31.5 ($ArCH_2$), 32.1 ($^t$Bu), 32.2 ($^t$Bu), 35.5 ($NCH_3$), 35.7 ($NCH_3$), 41.5 (α), 61.7 ($OCH_3$), 62.1 ($OCH_3$), 66.1 ($ImCH_2$), 66.2 ($ImCH_2$), 118.2, 124.4, 125.4, 125.5, 128.8, 130.5, 130.7, 130.8, 132.9, 133.2, 133.5, 136.5, 137.0, 137.1, 137.2, 138.7, 147.8, 149.8, 149.9, 153.0, 155.3, 155.5, 156.5. **ESI-MS** ($CH_3OH$) *m/z*: 1511.6 (calc. 1511.6 for $[Zn(\mathbf{2})+ClO_4]^+$)

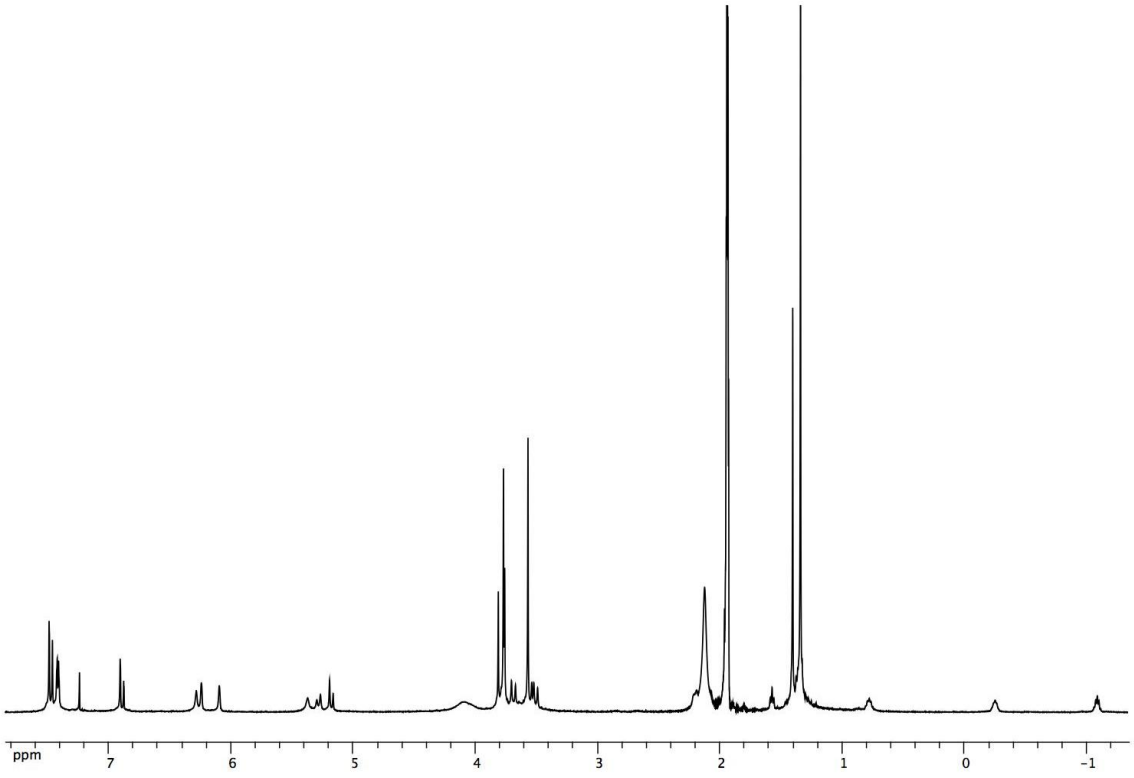


Figure S5. $^1$H NMR ($CD_3CN$, 500 MHz, 300 K) of $[Zn(\mathbf{2})](ClO_4)_2$

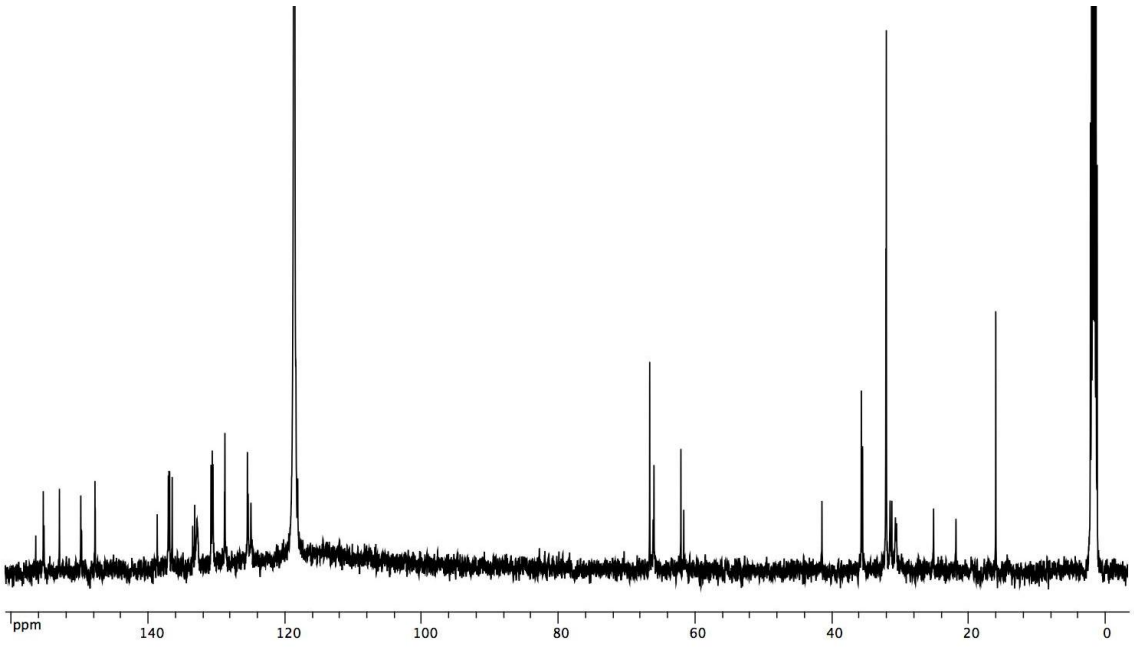


Figure S6. $^{13}$C NMR ($CD_3CN$, 125 MHz, 300 K) of $[Zn(\mathbf{2})](ClO_4)_2$

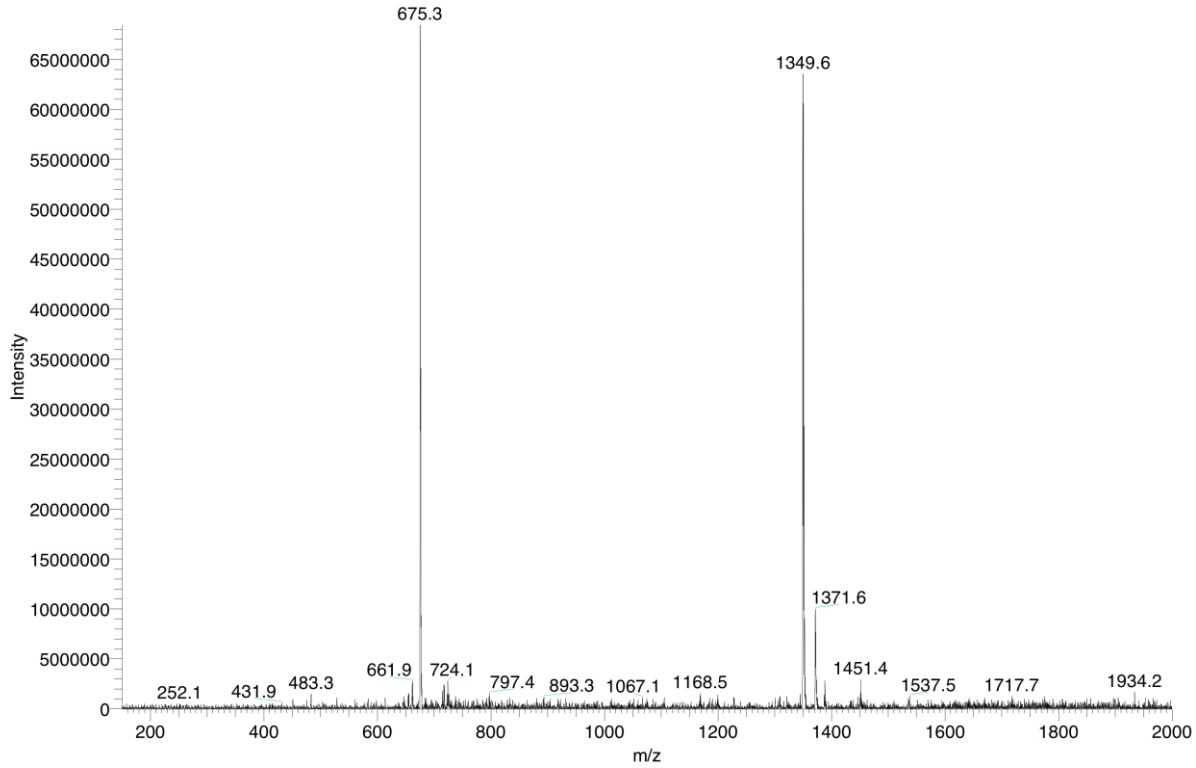


Figure S7 ESI-MS (positive ionization, $CH_3OH$) of ligand $M_{C4NH2}$, displaying peaks for $[(\mathbf{2})+H]^+$ (1349.6), $[(\mathbf{2})+Na]^+$ (1371.6) and $[(\mathbf{2})+2H]^{2+}$ (675.3).

2-b) Synthesis of $L_{C4NH2}^{TNpy}$

[Zn(**2**)]$(ClO_4)_2$ (280 mg, 173 μmol), N-propargyl-N-(2-pyridylmethyl)-methylamine (100 mg, 623 μmol), sodium ascorbate (179 mg, 900 μmol) and $CuSO_4 \cdot 5H_2O$ (112 mg, 0.450 μmol) were mixed in a vial. $CH_2Cl_2$ (3 mL) and $H_2O$ (3 mL) were stepwise added under Ar atmosphere. The mixture was stirred for 15 hours at room temperature. The residue was diluted with $CH_2Cl_2$ (25 mL) and water (25 mL), and chelex resin(3 mL) was added along with 10 drops of $NH_3$ 28%. The mixture was stirred in air for 1h. The organic layer was separated, and the aqueous phase extracted twice with $CH_2Cl_2$ (2×20 mL). The combined organic layers were washed with brine (20 mL), dried over $Na_2SO_4$, filtered, and evaporated. The brown solid was washed with $Et_2O$ (2x10 mL) and centrifuged yielding a brown powder (228 mg, 79%).

**$^1$H (with one equiv. Zn$^{II}$. 250 MHz, $CD_3CN$, 300 K)** δ (ppm): -1.13 (s, 2H, β), -0.90(s, 2H, γ), 0.61(s, 2H, δ), 0.79(s, 2H, α), 1.33 (s, 18H, *t*Bu), 1.41 (s, 9H, *t*Bu), 2.15 (br, 6H, $NMe_{large\ rim}$), 2.25 (br, 2H, $NH_2$), 3.56-4.20 (br, 16H, $CH_{2Tria}$ + $CH_2Ar$), 3.66 (s, 9H, OMe), 3.73 (s, 4H, $CH_2$py), 3.77 (s, 6H, $NMe_{Im}$), 3.84 (s, 3H, $NMe_{Im}$), 5.21 (d, 2H, J = 7.5 Hz, $CH_2$Im), 5.31 (d, 2H, J = 7.5 Hz, $CH_2$Im), 5.41 (s, 2H, $CH_2$Im), 6.21(s, 1H, $HAr_{Triachain}$), 6.54 (s, 1H, $H_{Triachain}$), 6.75 (s, 2H, $HAr_{Tria\ Npy}$), 6.92 (d, 1H, J < 1Hz, $H_{Im}$), 6.94 (d, 2H, J < 1Hz, $H_{Im}$), 7.03(s, 2H, $HAr_{Tria\ Npy}$), 7.20 (br, 2H, Hpy(meta)), 7.39 (br, 4H, HAr*t*Bu), 7.41(br, 2H, Hpy(meta')), 7.48 (br, 2H, HAr*t*Bu), 7.51(d, 2H, J < 1Hz, $H_{Im}$), 7.52 (d, 1H, J < 1Hz, $H_{Im}$), 7.55 (s, 2H, HTria Npy), 7.58(br, 2H, Hpy(para)), 7.70(br, 2H, Hpy(ortho)). **ESI-MS** ($CH_3OH$) *m/z*: 1670.9 (calc. 1669.9 for $[M+H]^+$), 836.0 (calc. 885.4 for $[M+2H]^{2+}$)

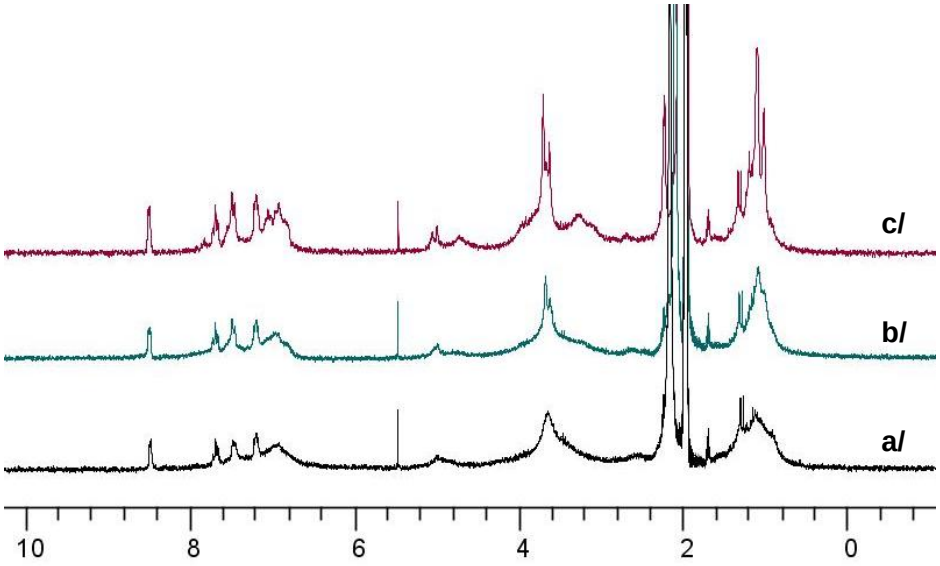


Figure S8. $^{1}$H NMR spectrum of $L_{C4NH2}^{TNpy}$ ($CD_3CN$, 250 MHz). a/ 300K, b/ 320K, c/ 340K.

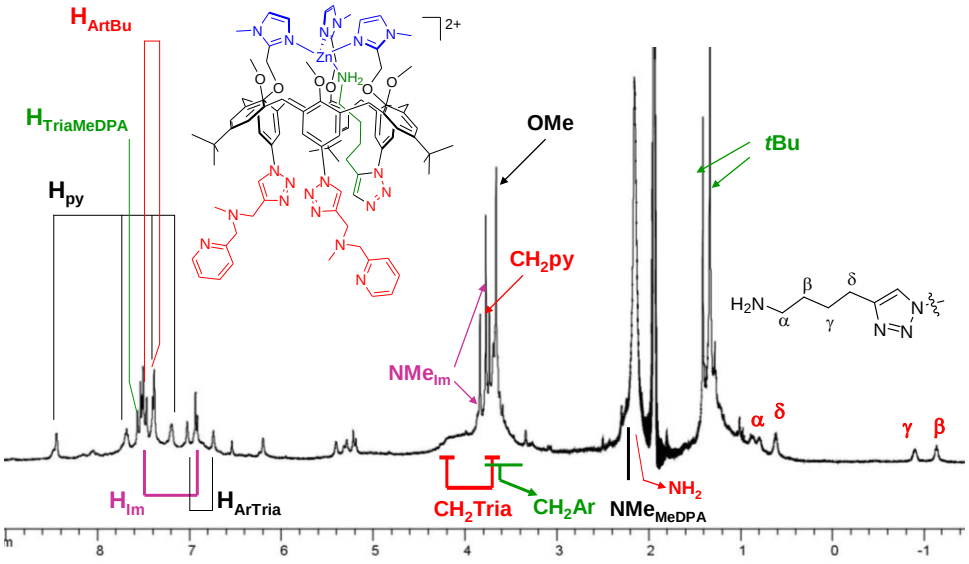


Figure S9. $^{1}$H NMR spectrum ($CD_3CN$, 250 MHz, 300 K) of $L_{C4NH2}^{TNpy}$ $Zn(ClO_4)_2$ Attribution of the peaks based on COSY and HSQC experiments. The amino side chain is autocoordinated as evidenced by the upfield shifts of corresponding resonances (α, β, γ, δ and $H_{Triachain}$)

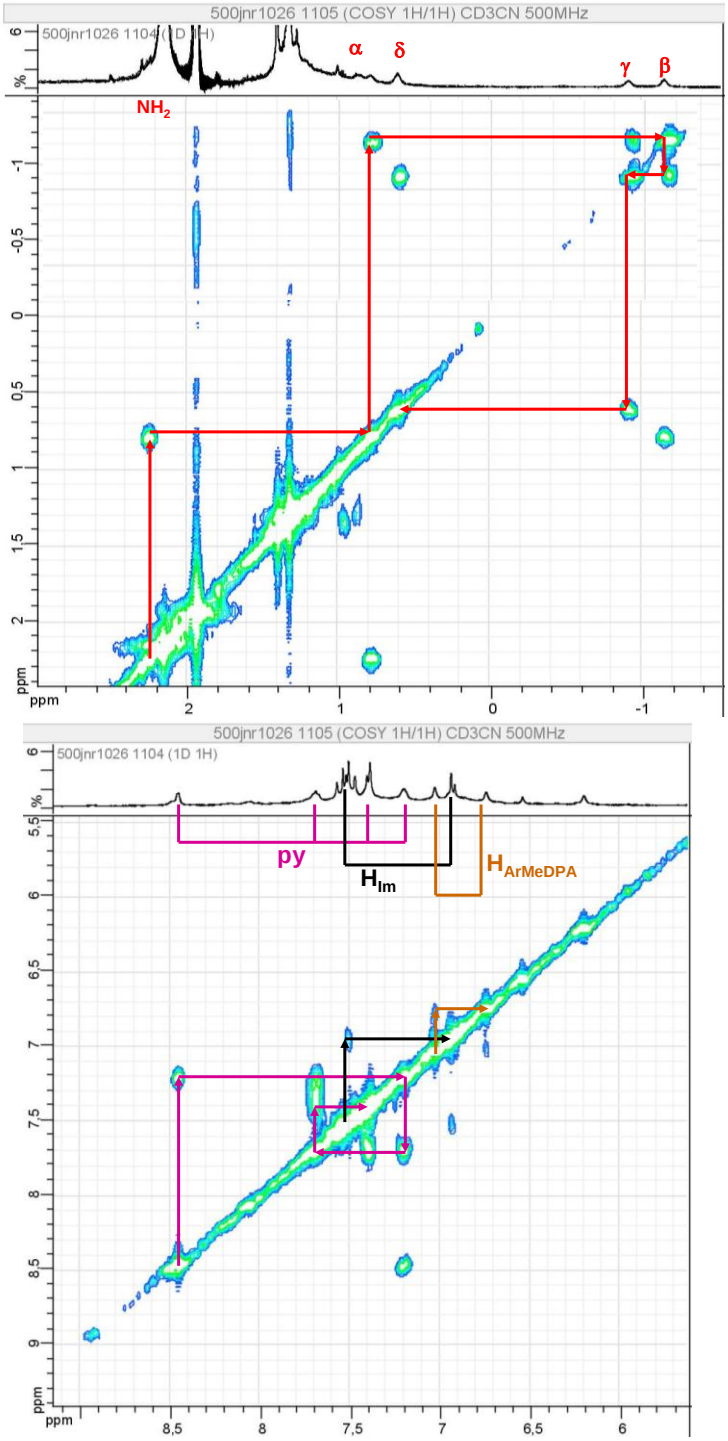


Figure S10. COSY spectrum ($CD_3CN$, 250 MHz, 300 K) of $L_{C4NH2}^{TNpy}$ $Zn(ClO_4)_2$

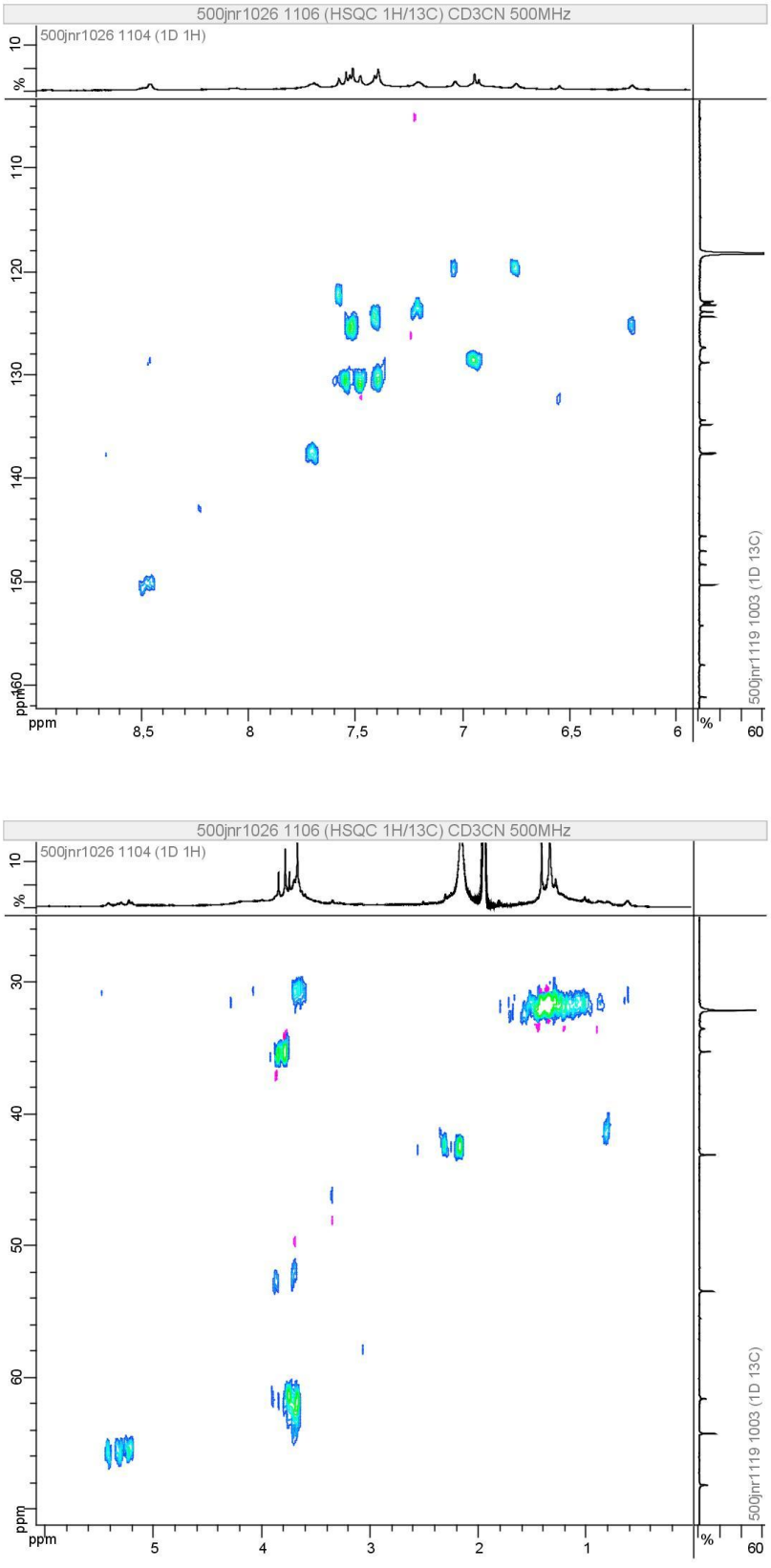


Figure S11. HSQC spectrum($CD_3CN$, 250 MHz, 300 K) of $L_{C4NH2}^{TNpy}$ $Zn(ClO_4)_2$

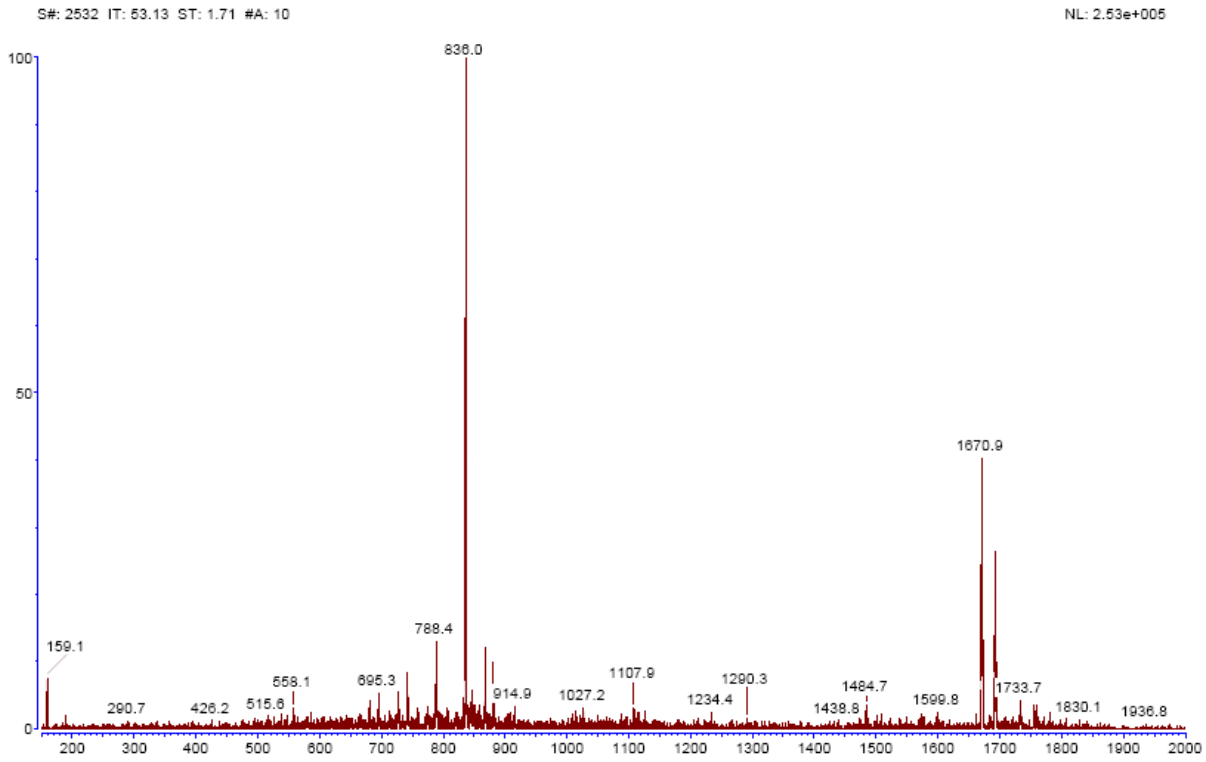


Figure S12. ESI-MS spectrum of $L_{C4NH2}^{TNpy}$ ([M+H]$^+$ at 1670.9 and [M+2H]$^{2+}$ at 836).

*2-c) Synthesis of* $L_{C4NHBoc}^{TNpy}$

$L_{C4NH2}^{TNpy}$ (228 mg, 136 µmol) was dissolved in dry THF. The solution was cooled to 0°C. $Et_3N$ (28 µL, 205 µmol) and $Boc_2O$ (44.7 mg, 205 µmol) were added and the solution was stirred at room temperature overnight. The solvent was then removed under vacuum, and the residue was taken in $CH_2Cl_2$ (20 mL) and a saturated $NH_4Cl$ aqueous solution (20 mL). After separation, the aqueous phase was extracted twice with $CH_2Cl_2$ (2×10 mL). The combined organic layers were dried with $Na_2SO_4$, filtered, and $CH_2Cl_2$ was evaporated. The tan solid was washed with $Et_2O$ (2x10 mL), centrifuged, filtered and dried (206 mg, 85%)
**$^1$H(500 MHz, DMSO d$^6$, 300 K)** relatively broad spectrum**. $^1$H (with two equiv. Zn$^{II}$. 500 MHz, CD$_3$CN, 275 K)** δ (ppm): 0.95 (s, 9H, HtBu), 1.33 (m, 20H, 18HtBu + 2H$_\gamma$), 1.39 (m, 11H, 9HtBu + 2H$_\beta$), 1.75 (s, 3H, HNMe$_{Npy}$), 2.04 (s, 3H, HNMe$_{Npy}$), 2.42 (m, 2H, H$_\delta$), 2.92 (m, 2H, H$_\alpha$), 3.40 (m, 2H, CH$_{2Ar}$), 3.75-3.56 (m, 22H, 4HCH$_{2Ar}$ + 9HOMe + 9HNMe$_{Im}$), 4.04 (m, 4H, 2HCH$_{2py}$ + 2HCH$_{2Ar}$), 4.24 (s, 2H, HCH$_{2py}$), 4.33 (m, 2H, HCH$_{2Ar}$), 4.49 (m, 2H, HCH$_{2Ar}$), 4.57 (m, 2H, CH$_{2TriaNpy}$), 5.35-4.89 (m, 6H, HCH$_{2Im}$), 5.77 (s, 1H, H$_{ArNpy}$), 6.30 (s, 1H, H$_{Archain}$), 6.52 (s, 1H, H$_{ArNpy}$), 6.62 (s, 1H, H$_{Archain}$), 6.74 (s, 1H, H$_{ArNpy}$), 6.90 (s, 1H, H$_{Im}$), 6.91 (s, 1H, H$_{Im}$), 7.05 (s, 1H, H$_{Im}$), 7.10 (s, 1H, H$_{ArtBu}$), 7.14 (m, 1H, Hpy *endo)*, 7.18 (s, 1H, H$_{ArNpy}$), 7.46-7.34 (m, 8H, 2H$_{Im}$+5H$_{ArtBu}$+1Hpy *endo*), 7.51 (s, 2H, H$_{NHBoc}$+H$_{Im}$), 7.55 (m, 1H, Hpy *exo)*, 7.63 (m, 1H, Hpy *endo)*, 7.73 (m, 1H, Hpy *exo)*, 7.82 (s, 1H, H$_{Tria\ Npy}$*)*, 7.84 (s, 1H, H$_{Tria\ Npy}$*)*, 8.05 (m, 1H, Hpy *exo)*, 8.19 (m, 1H, Hpy *endo)*, 8.93 (m, 1H, Hpy *exo).*
**$^{13}$C (125 MHz, DMSO d$^6$, 300 K)** δ (ppm): 22.87(δ), 24.53(γ), 28.21(β), 28.98(ArCH$_2$), 30.85($^t$Bu), 32.63($^t$Bu), 33.61(NCH$_{3Im}$), 41.77(α), 51.74 (CH2Tria), 59.85 (OMe), 62.40 (CH$_2$py), 65.96 (CH2Im), 117.98, 121.79, 122.11, 122.68, 123.25, 127.14, 128.27, 131.19, 132.04, 133.17, 135.12, 135.4, 136.41, 144.98, 145.66, 148.66, 150.93, 155.51, 155.99, 157.17, 158.89 **ESI-MS** (CH$_3$OH) *m/z*: 1770.9 (calc. 1771.0 for [M+H]$^+$), 886.0 (calc. 886.0

for $[M+2H]^{2+}$) **HR-MS**. Peak at 1770.0060 corresponds to the formula $C_{103}H_{124}N_{20}O_8$ in agreement with [ $L^{TNpy}_{C4NHBoc}$ + $H]^+$ (mass error: 4.0 ppm).

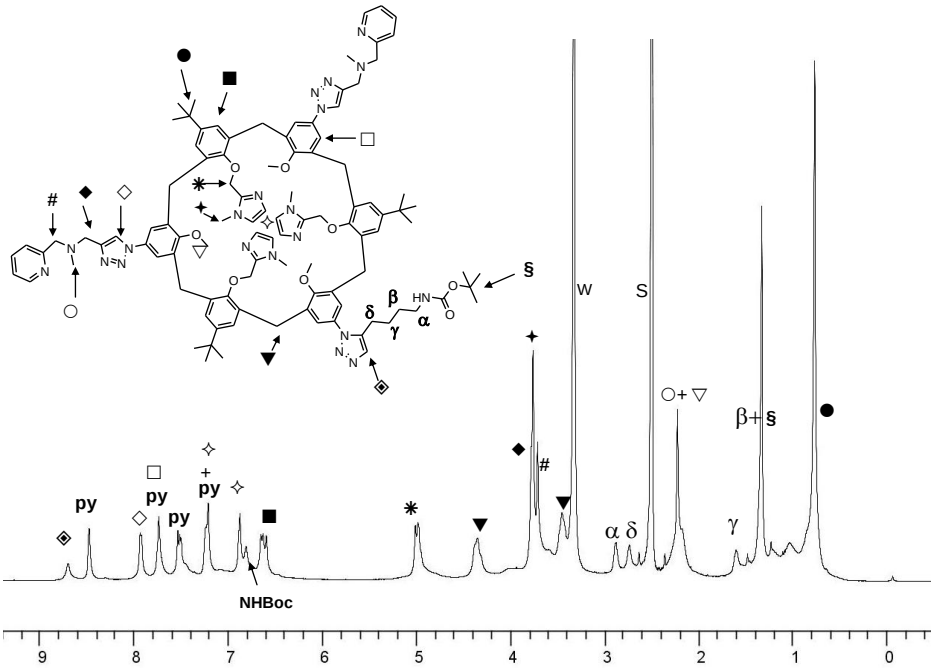


Figure S13. $^1$H NMR spectrum (DMSO, 500 MHz, 300 K) of $L^{TNpy}_{C4NHBoc}$.

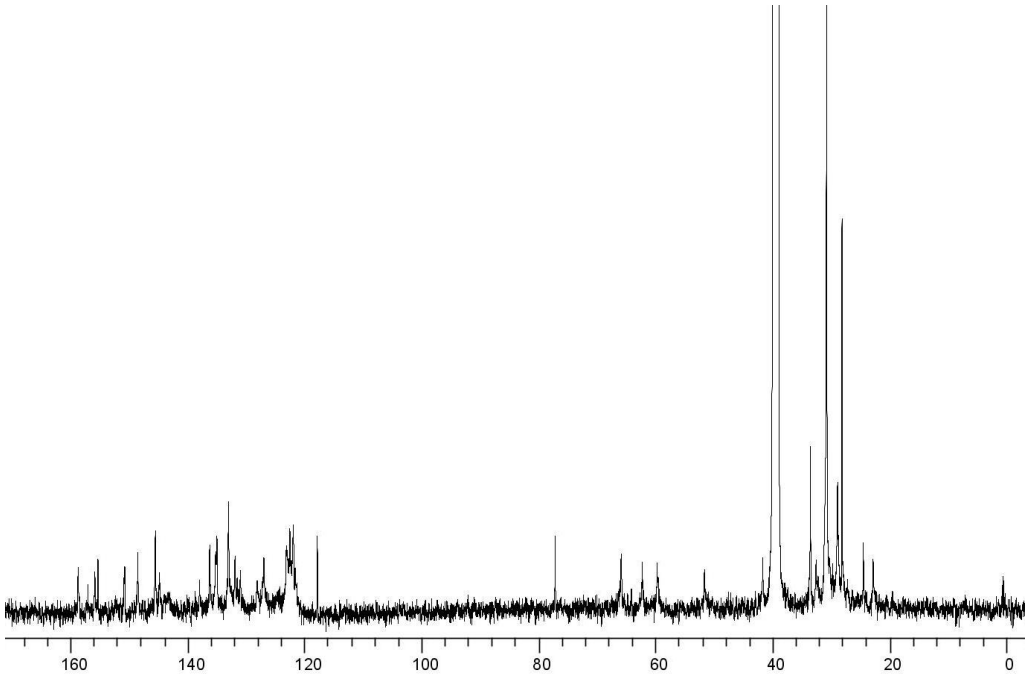


Figure S14. $^{13}$C NMR spectrum (DMSO, 500 MHz, 300 K) of $L^{TNpy}_{C4NHBoc}$

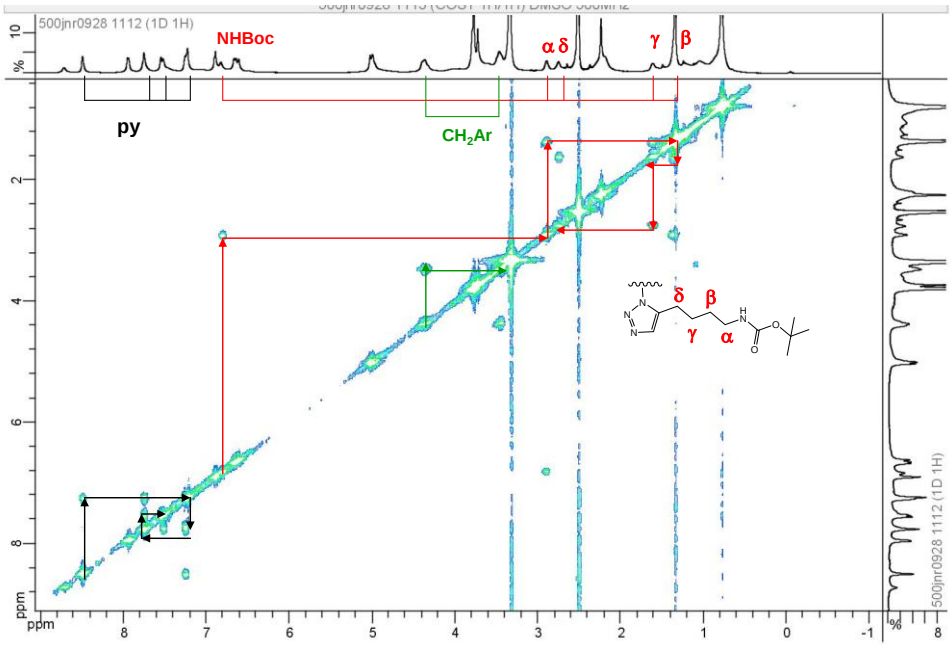


Figure S15. COSY (DMSO, 500 MHz, 300 K) of $L_{C4NHBoc}^{TNpy}$

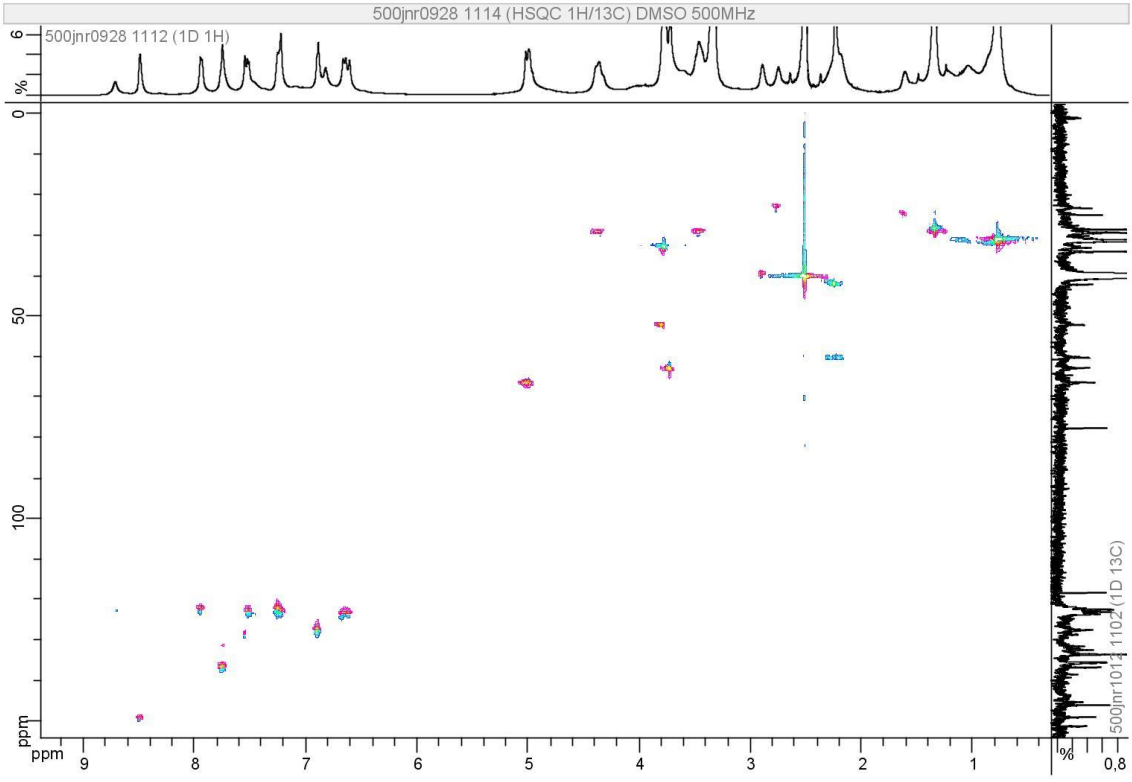


Figure S16. HSQC (DMSO, 500 MHz, 300 K) of $L_{C4NHBoc}^{TNpy}$

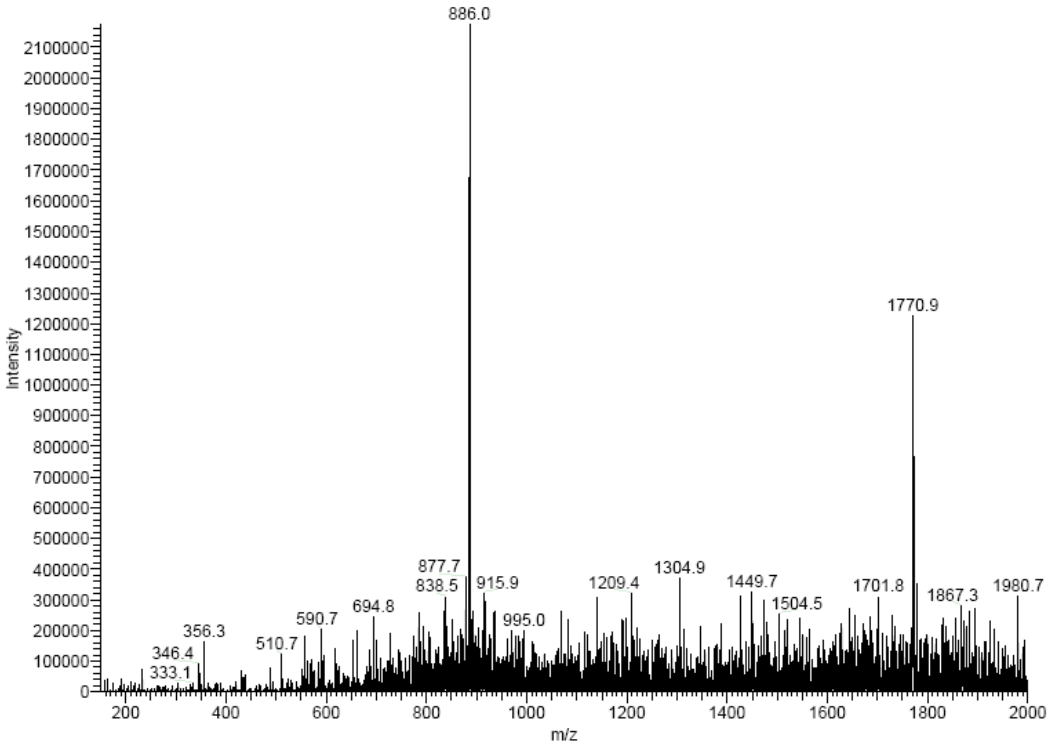


Figure S17. ESI-MS (MeOH) spectrum of $L^{TNpy}_{C4NHBoc}$ (([M+H]$^{+}$ at 1770.9 and [M+2H]$^{2+}$ at 886).

***3) Spectroscopic characterization of the mononuclear Zn complexes***

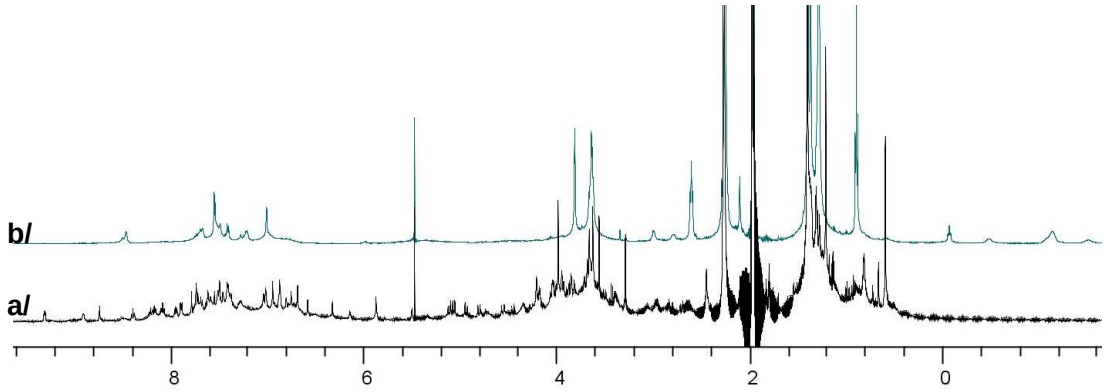


Figure S18. $^{1}$H spectra ($CD_3CN$, 500 MHz, 275 K) of: a/ $L^{TNpy}_{C4NHBoc}$ +1 eq Zn ; b/ $L^{TNpy}_{C4NHBoc}$ +1 eq Zn + 2 eq heptylamine.

## ***4) Spectroscopic characterization of the dinuclear Zn complexes***

General procedure for the preparation of dinuclear $Zn^{II}$ complexes of $L^{TNpy}$ and $L^{TNpy}_{C4NHBoc}$

L (7.5 µmol) and $Zn(CF_3SO_3)_2$ (15 µmol) were mixed in $CH_3CN$ (0.5 mL) and precipitated with diethylether (4 mL). After centrifugation, the solid is dried under vacuum.

A tetracationic complex is obtained with $L^{TNpy}_{C4NHBoc}$ (yield ρ = 63%) whereas a pentacationic one is obtained with $L^{TNpy}$ (yield ρ = 75%) as confirmed by elemental analysis (see below). This is ascribed to the protonation of the dangling teriary amine of $L^{TNpy}$ , which is absent from $L^{TNpy}_{C4NHBoc}$.

Elemental analysis:

**$L^{TNpy}Zn_2(MeCN)(CF_3SO_3)_4(CF_3SO_3H)(H_2O)_3$**

Found: C 48.63; H 4.82; N 11.02. Calculated for $L^{TNpy}Zn_2(MeCN)(CF_3SO_3)_4(HCF_3SO_3)(H_2O)_3$ : C 48.39; H 4.73; N 11.39.

**$L^{TNpy}_{C4NHBoc}Zn_2(MeCN)(CF_3SO_3)_4(H_2O)(Et_2O)_3$**

Found: C 52.57; H 5.46; N 10.53. Calculated for [$L^{TNpy}_{C4NHBoc}Zn_2(MeCN)(CF_3SO_3)_4$](H₂O)(Et₂O)₃: C 52.30; H 5.77; N 10.59.

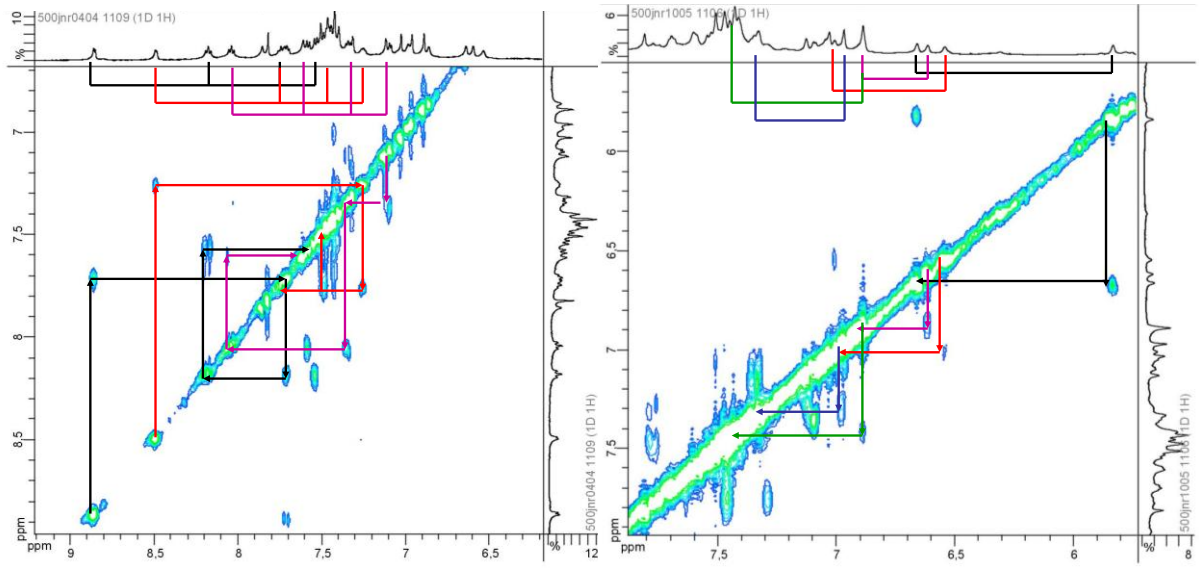


Figure S19. COSY spectrum of $L^{TNpy}Zn_2(MeCN)(ClO_4)_4$ ($CD_3CN$, 500 MHz, 265 K).Correlations between pyridyl protons (left) evidence the presence of three sets of protons. The red correspond to the unbound pyridyl. The black set corresponds to the bound pyridyl oriented outside the cavity. The purple set corresponds to the bound pyridyl oriented inside of the cavity and submitted to the shielding effect of the calixarene walls. Correlations between other aromatics (right) reflect the dissymmetry of the molecule (in Cs group).

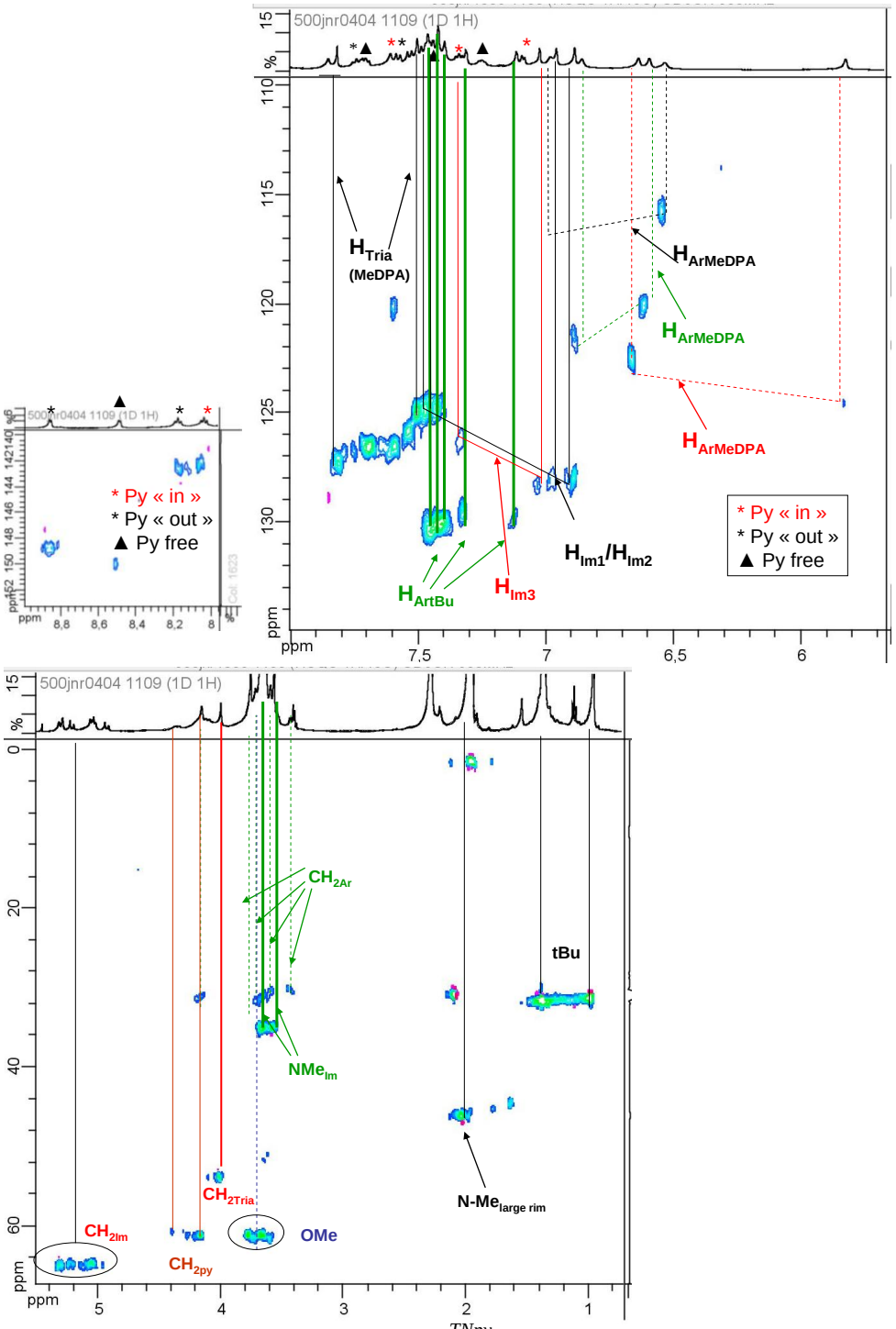


Figure S20. HSQC spectrum of $L^{TNpy}Zn_2(MeCN)(ClO_4)_4$ ($CD_3CN$, 500 MHz, 275 K). The symmetry of the system is not exactly Cs, but $C_1$. Indeed, the large rim complex is not perfectly symmetrical with respect to the planar symmetry (π) because of the helicity of the large rim complex. On the NMR spectrum, this lowering of symmetry (Cs to $C_1$) is felt essentially by groups located near the source of symmetry breaking (i.e. the large rim complex). As a consequence, the *t*Bu groups and their corresponding aromatic units, which are rejected outside the cavity, each appear as two sets of signals in a 1:2 ratio (apparent Cs symmetry). For the same reasons, the protons present at the small rim ($H_{Im}$, $CH_{2Im}$) display signals expected for a Cs symmetry. On the other hand, the aromatic units bearing the triazole groups, which are forced inside the cavity, sense a $C_1$ symmetry that is reflected in the

complete splitting of their resonances). Their inner position also explains the noticeable shielding they encounter.

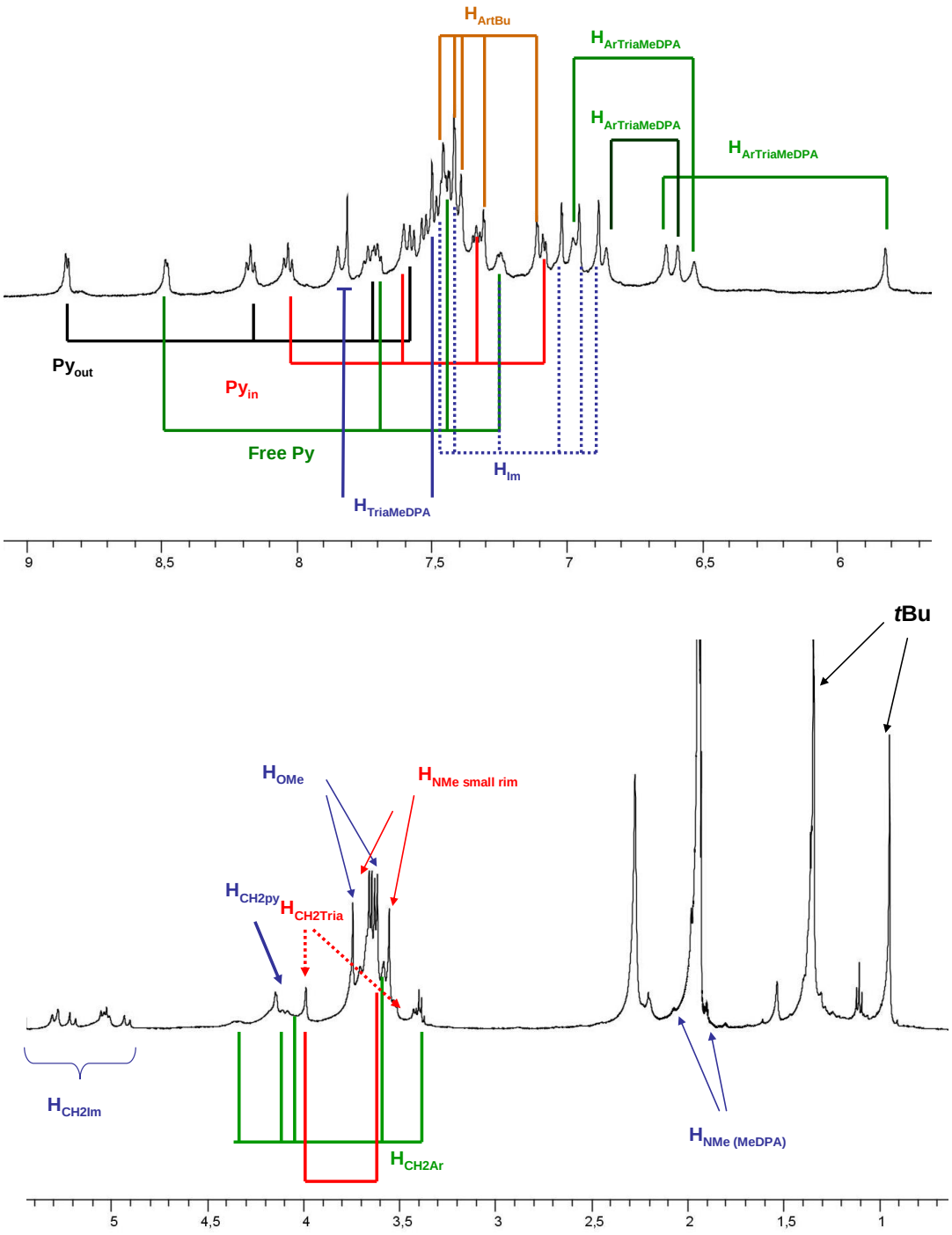


Figure S21. $^{1}$H spectrum of $L^{TNpy}Zn_2(MeCN)(ClO_4)_4$ ($CD_3CN$, 500 MHz, 275 K). Attribution of all proton resonances.

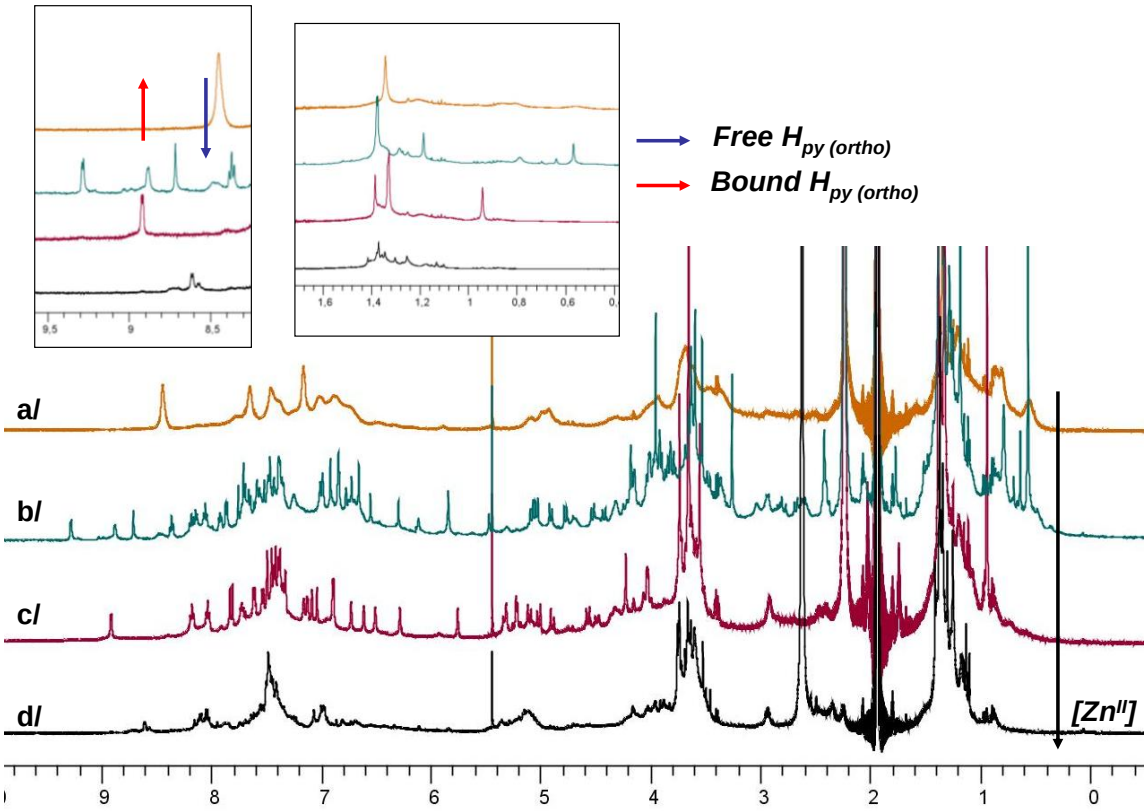


Figure S22. Titration of $L^{TNpy}_{C4NHBoc}$ with $Zn^{II}$ (triflate counterion). a/ $L^{TNpy}_{C4NHBoc}$; b/ $L^{TNpy}_{C4NHBoc}$ + 1 eq. $Zn^{II}$; c/ $L^{TNpy}_{C4NHBoc}$ + 2 eq. $Zn^{II}$; d/ $L^{TNpy}_{C4NHBoc}$ + 3 eq. $Zn^{II}$; ($CD_3CN$, 500 MHz, 275K). Inserts: zoom on the region of the ortho proton resonance of pyridyl (bound and unbound regions are indicated by the colored arrows) and on the *tert*butyl resonances of the ligand.

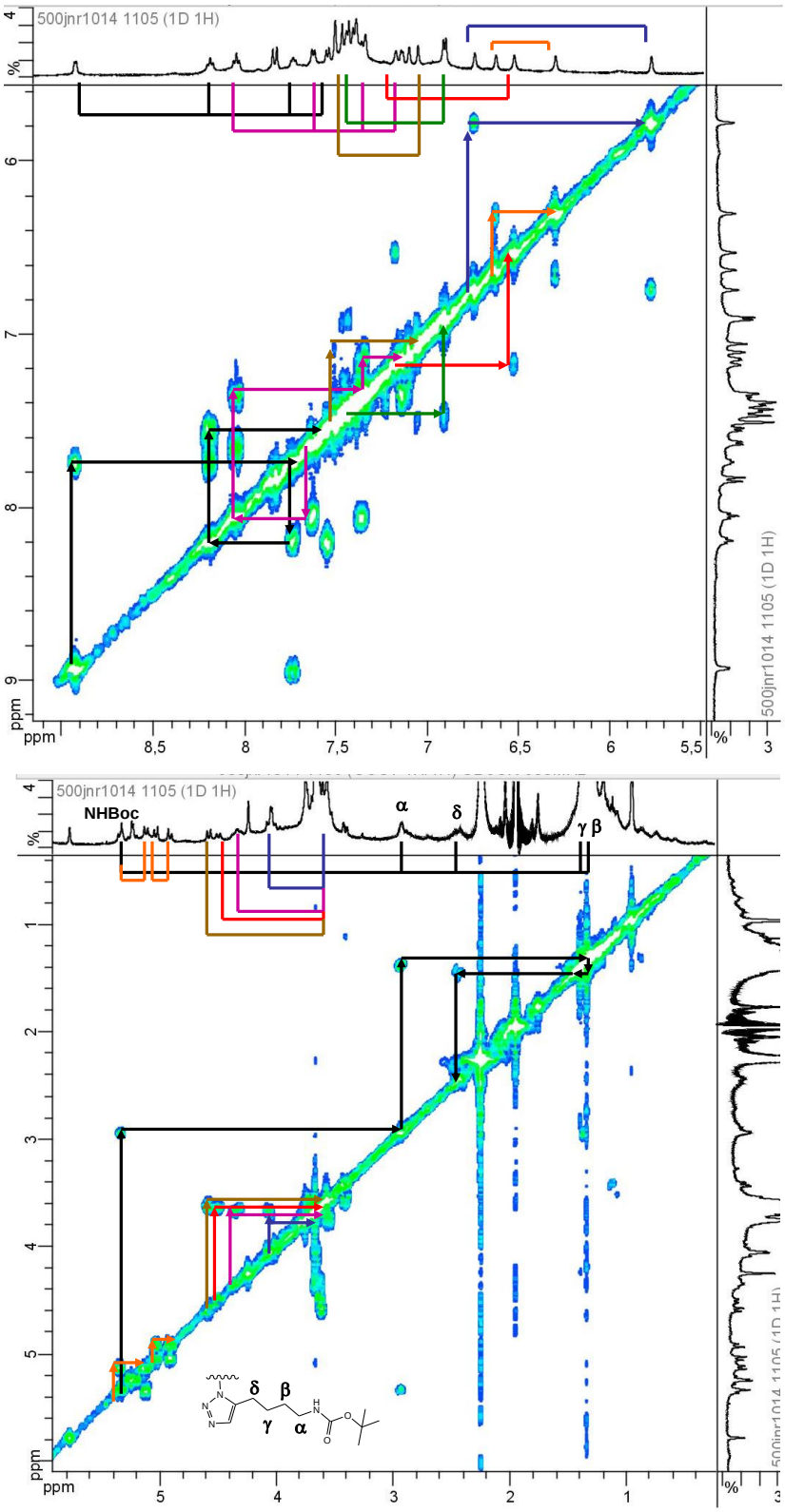


Figure S23. COSY spectrum of $L^{TNpy}_{C4NHBoc}$ $Zn_2(MeCN)(ClO_4)_4$ ($CD_3CN$, 500 MHz, 275 K).Correlations between pyridyl protons (left) evidence the presence of three sets of protons. The black set corresponds to the bound pyridyl oriented outside the cavity. The purple set corresponds to the bound pyridyl oriented inside of the cavity and submitted to the shielding effect of the calixarene walls. Correlations between other aromatics (right) reflect the dissymmetry of the molecule (in Cs group).

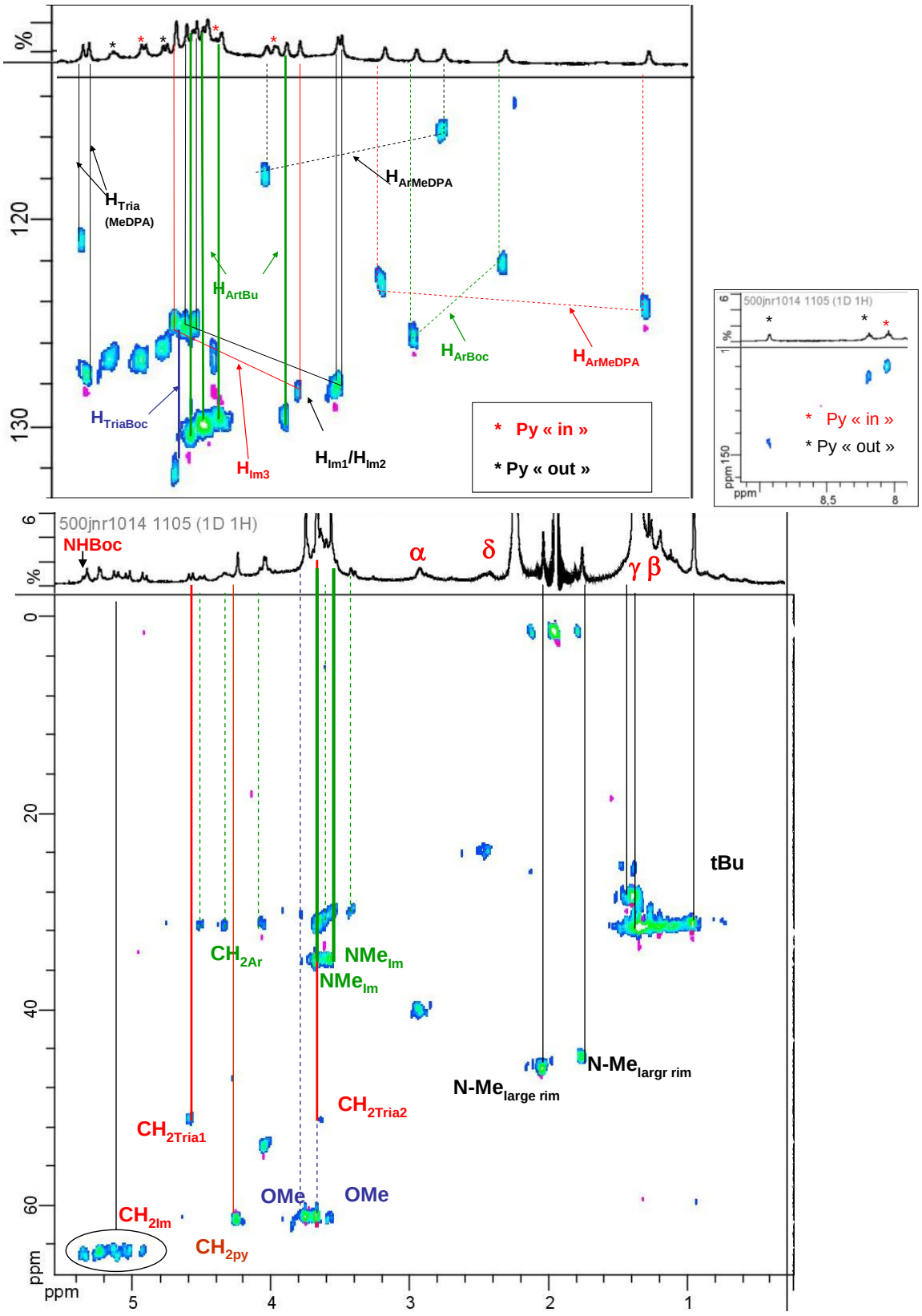


Figure S24. HSQC spectrum of $L^{TNpy}_{C4NHBoc}$ $Zn_2(MeCN)(ClO_4)_4$ ($CD_3CN$, 500 MHz, 275 K).

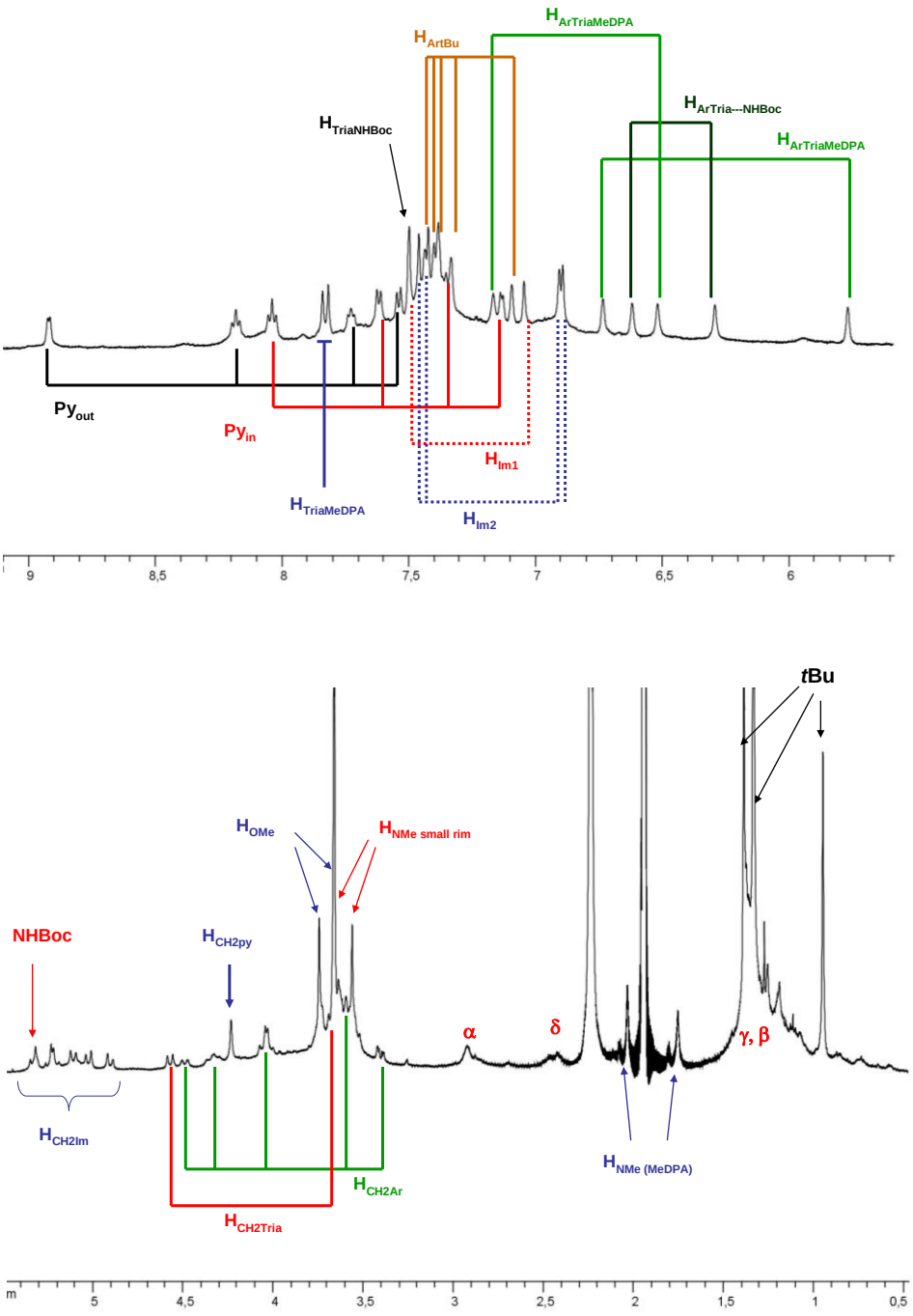


Figure S25. $^{1}$H spectrum of $L^{TNpy}_{C4NHBoc}$ $Zn_2(MeCN)(ClO_4)_4$ ($CD_3CN$, 500 MHz, 275 K). Attribution of all proton resonances.

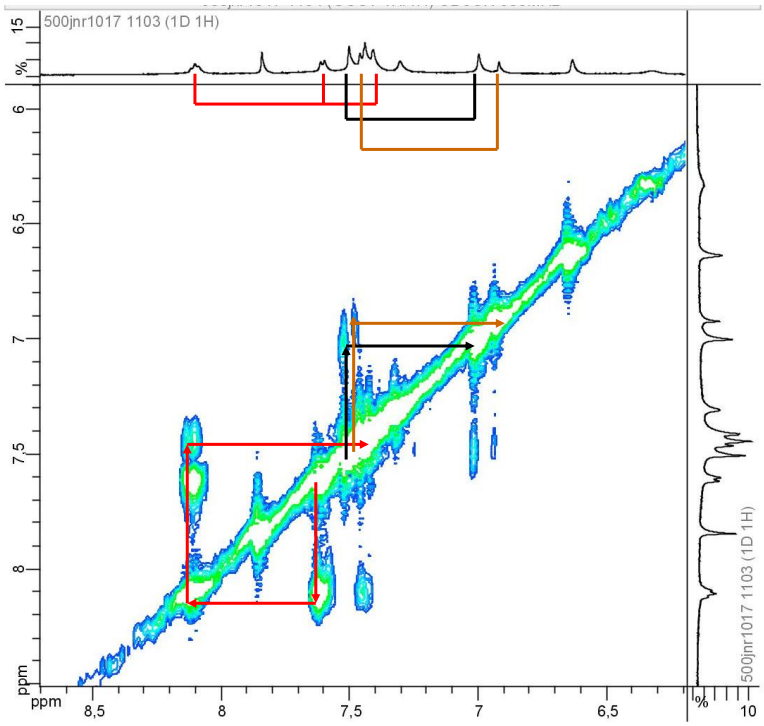


Figure S26. COSY spectrum of $L^{TNpy}_{C4NHBoc}$ $Zn_2(MeCN)(ClO_4)_4$ ($CD_3CN$, 500 MHz, 340 K).

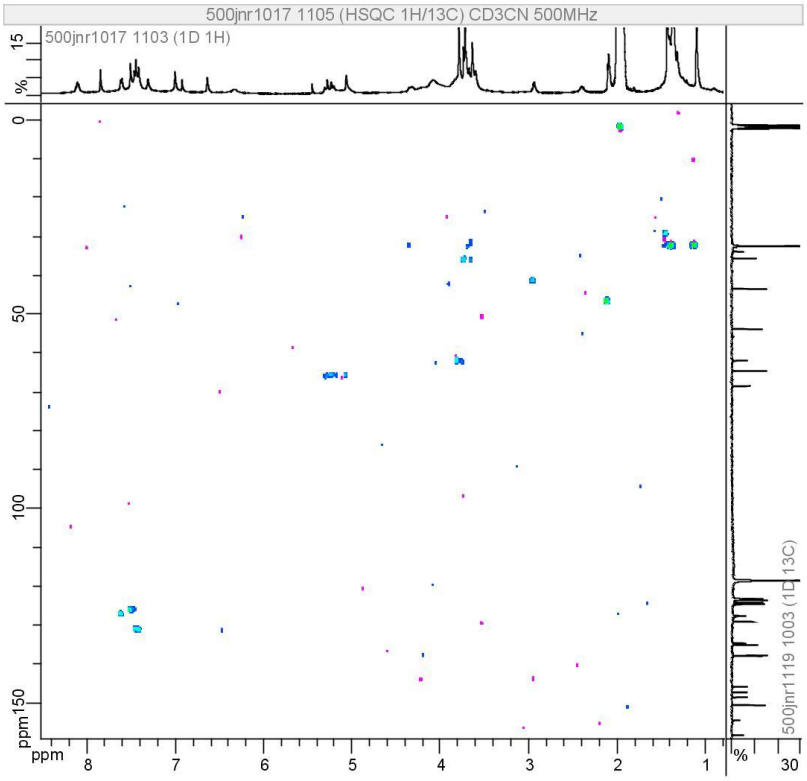


Figure S27. HSQC spectrum of $L^{TNpy}_{C4NHBoc}$ $Zn_2(MeCN)(ClO_4)_4$ ($CD_3CN$, 500 MHz, 340 K).

| | $L^{TNpy}_{C4NHBoc}$ (340K) | $L^{TNpy}_{C4NHBoc}$ $Zn_2(MeCN)(ClO_4)_4$ (275 K) | $L^{TNpy}_{C4NHBoc}$ $Zn_2(MeCN)(ClO_4)_4$ (340 K) |
|---|---|---|---|
| $CH_{2Tria}$ | 3,67 | 4,58 /4,05<----> 3,65 | / |
| $CH_{2py}$ | 3,74 | 4,24 | 4,05 |
| N-Me (large rim) | 2,24 | 2,03 / 1,74 | 2,10 |
| $H_{Tria}$ | 7,81 | 7,81/7,84 | 7,84 |
| $CH_{2Im}$ | 4,67-4,99 (m) | 4,89-5,33 (m) | 5,05-5,20 |

Table S1. Selected resonances of $L^{TNpy}_{C4NHBoc}$ and $L^{TNpy}_{C4NHBoc}$ $Zn_2(MeCN)(ClO_4)_4$ ($CD_3CN$, 500MHz), attributed by HSQC experiments. Large rim coordination impacts on the pyridyl resonances, and shifts the $CH_{2Tria}$, $H_{Tria}$, and $CH_{2py}$ resonances downfield. The same should be expected for the N-Me resonances, but a small upfield shift is observed. This might be ascribed to the location of this methyl group in the proposed octahedral complex. (i.e. in the shielding cone of aromatic ring of the bound pyridyl).

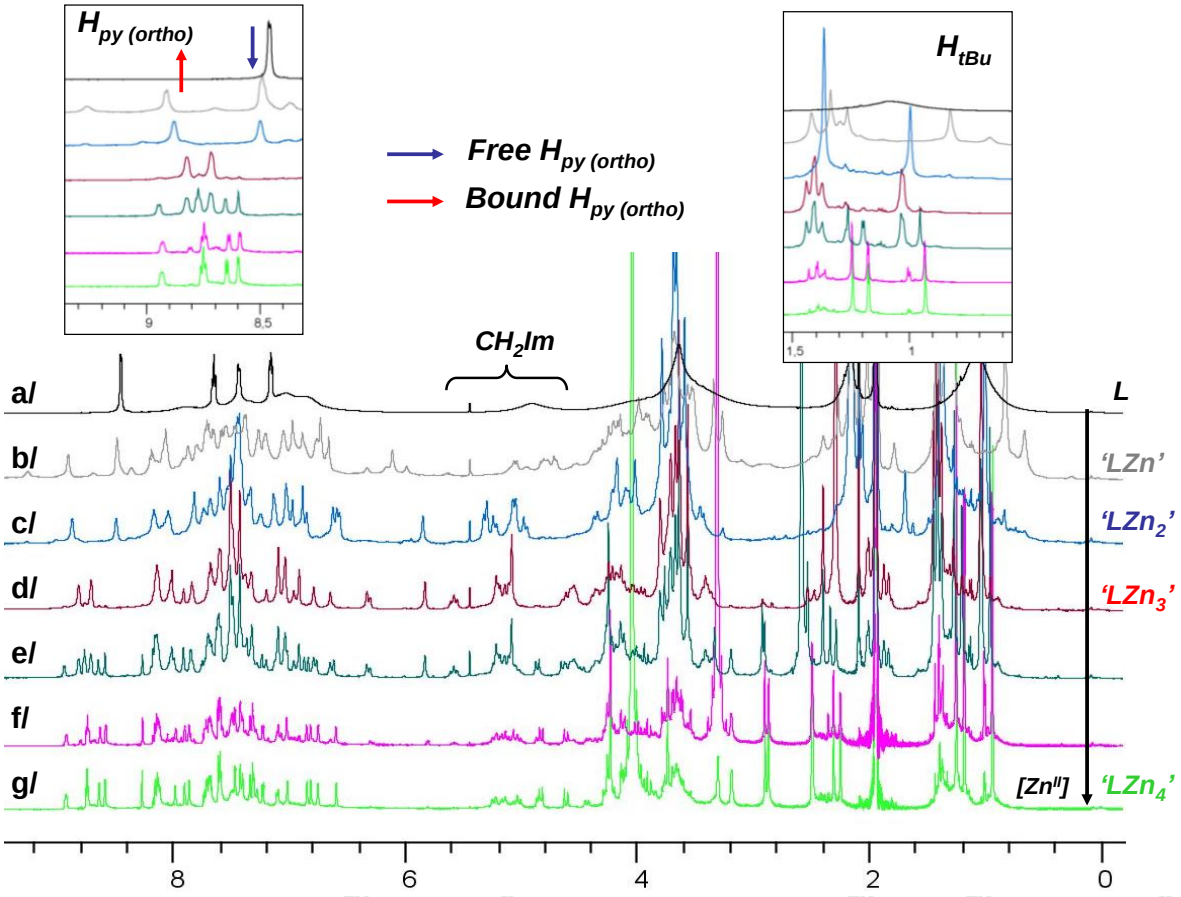


Figure S28. Titration of $L^{TNpy}$ with $Zn^{II}$ (triflate counterion). a/ $L^{TNpy}$; b/ $L^{TNpy}$ + 1 eq. $Zn^{II}$; c/ $L^{TNpy}$ + 2 eq. $Zn^{II}$; d/ $L^{TNpy}$ + 3 eq. $Zn^{II}$; e/ $L^{TNpy}$ + 4 eq. $Zn^{II}$ f/ $L^{TNpy}$ + 8 eq. $Zn^{II}$; g/ $L^{TNpy}$ + 15 eq. $Zn^{II}$ ($CD_3CN$, 500 MHz, 300K). Inserts: zoom on the region of the ortho proton resonance of pyridyl (bound and unbound regions are indicated by the colored arrows) and on the *tert*butyl resonances of the ligand. '$LZn_x$' stands for the $Zn^{II}$ complex of $L^{TNpy}$ of nuclearity x.

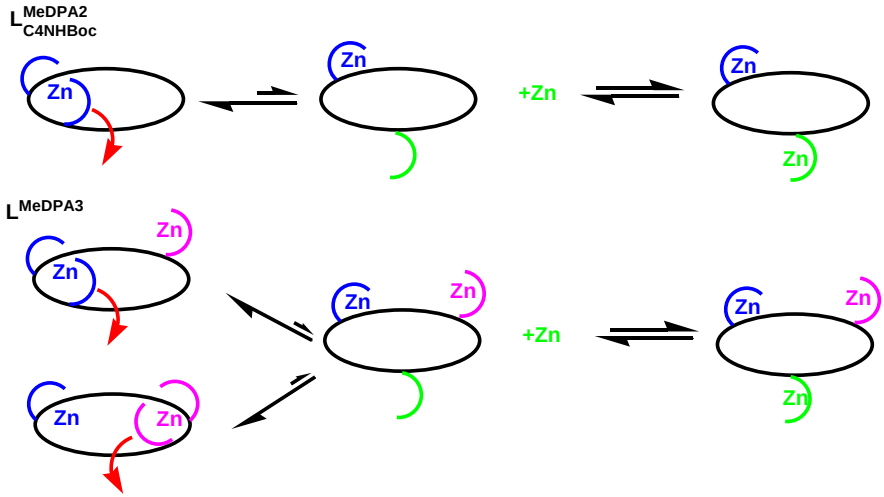


Figure S29 : Schematic view of the different complexation equilibria at the large rim involving the breaking of the octahedral complex.

While one equivalent is enough to break the octahedral complex of $L^{TNpy}_{C4NHBoc}$, more than four are necessary to form this new, presumably tetranuclear, complex with $L^{TNpy}$. This might be explained by statistical reasons. In order to bind an extra Zn, one of the the tridentate ligand of the octahedral complex has to decoordinate. With $L^{TNpy}_{C4NHBoc}$, it results in a competition of this ligand between the free Zn ion and the bound one. With $L^{TNpy}$, the competition occurs between the free Zn ion and the two bound Zn centers. For statistical reasons, coordination of the last metal ion becomes less favorable with $L^{TNpy}$.

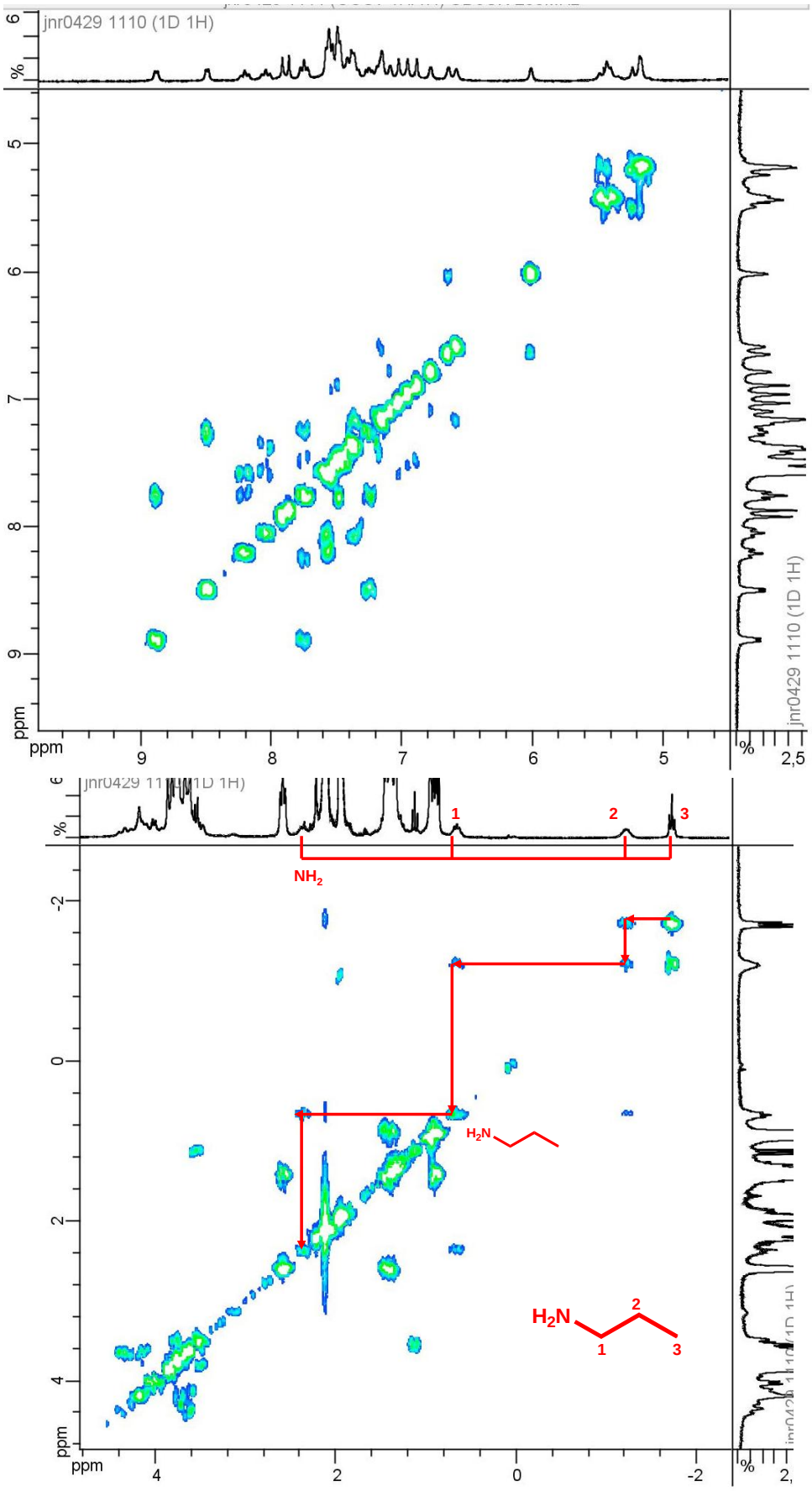


Figure S30. COSY spectrum ($CD_3CN$, 500 MHz, 275 K) of $L^{TNpy}Zn_2$(Propylamine)$(ClO_4)_4$ ($L^{TNpy}$ + 2 eq Zn + 4 eq propylamine).

***5) Spectroscopic characterization of the polynuclear Zn complex (nuclearity n > 2)***

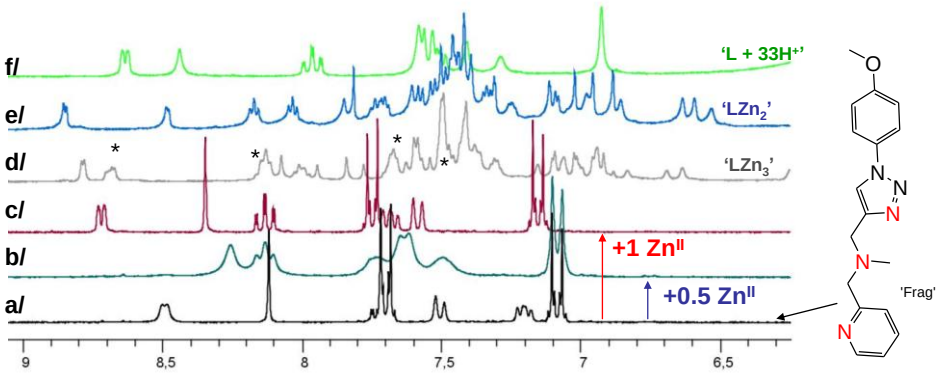


Figure S31. Comparison of the $L^{TNpy}Zn_3(MeCN)(ClO_4)_6$ spectrum with relevant spectra in $CD_3CN$. a/ tridentate fragment deprived of cavity,'Frag'; b/ 'Frag' +0.5 equiv. $Zn^{II}$; c/ 'Frag' +1 equiv. $Zn^{II}$; d/ $L^{TNpy}Zn_3(MeCN)(ClO_4)_6$ ; e/ $L^{TNpy}Zn_2(MeCN)(ClO_4)_4$ f/ $L^{TNpy}$ + 33 equiv. $H^+$ (trifluoroacetic acid). Spectra a/, b/ c/ f/: 250 MHz, 300 K. Spectra d/, e/: 500 MHz, 265 K. Spectrum c/ is a reference for the '*mono-TNpy*' binding mode to $Zn^{II}$. Comparison with spectrum d/ indicates that the 'dangling" pyridyl protons (*) appear at the same chemical shifts as in the bound fragment, evidencing a similar binding mode.The triazole resonance is upfield shifted (no signal at 8.3 ppm, as in spectrum c/) due to the shielding effect of the cavity.

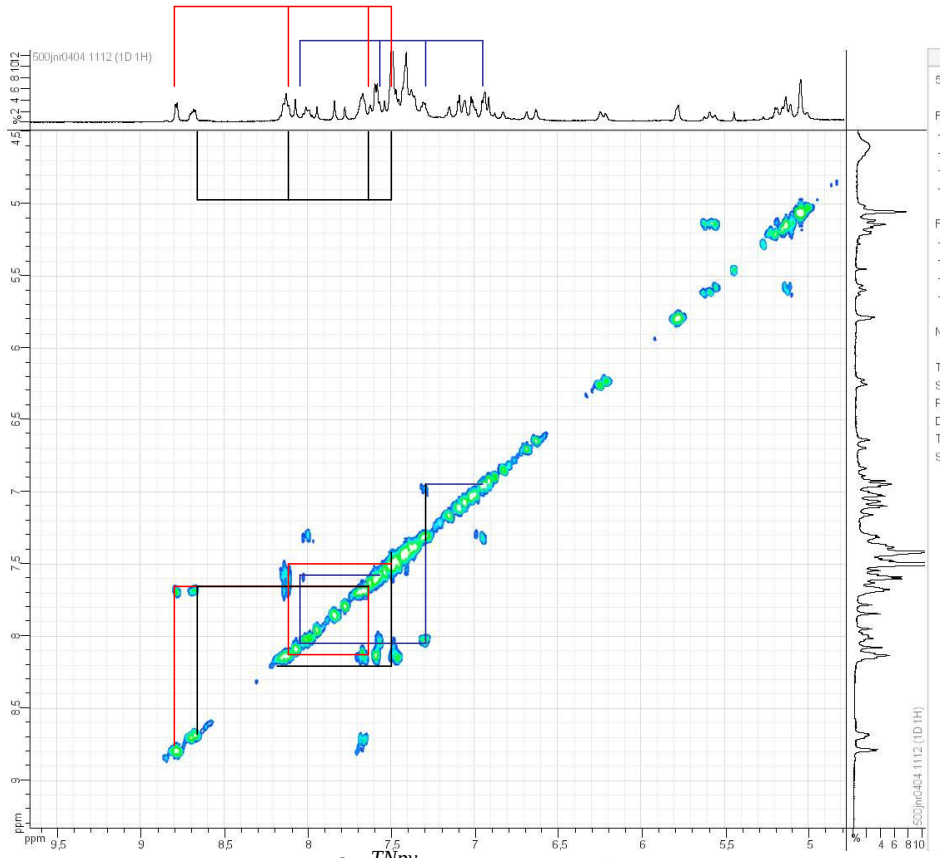


Figure S32. COSY spectrum of $L^{TNpy}Zn_3(MeCN)(ClO_4)_6$ ($CD_3CN$, 500 MHz, 265 K).

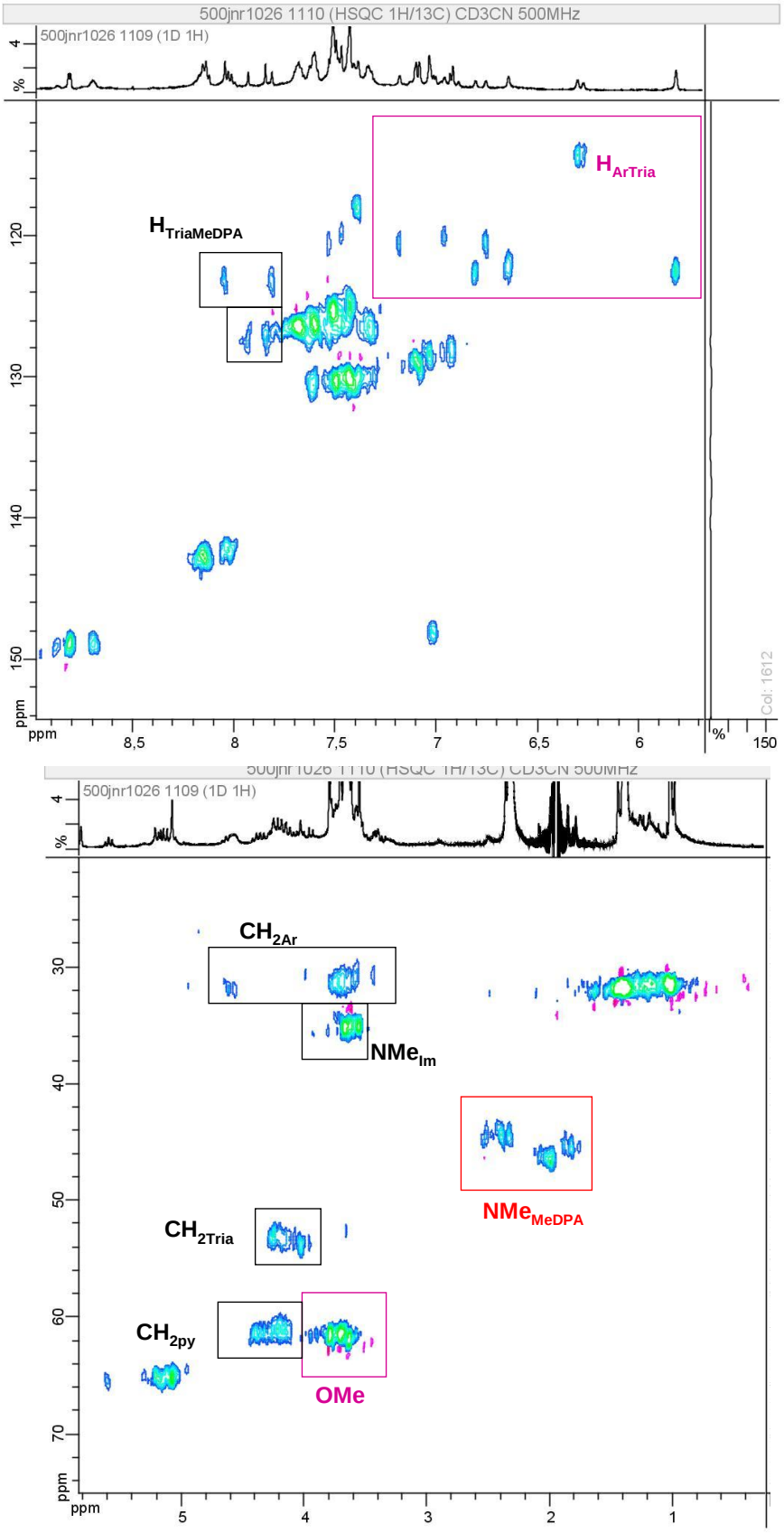


Figure S33. HSQC spectrum of $L^{TNpy}Zn_3(MeCN)(ClO_4)_6$ ($CD_3CN$, 500 MHz, 285 K).

## *6) Supramolecular control of nuclearity*

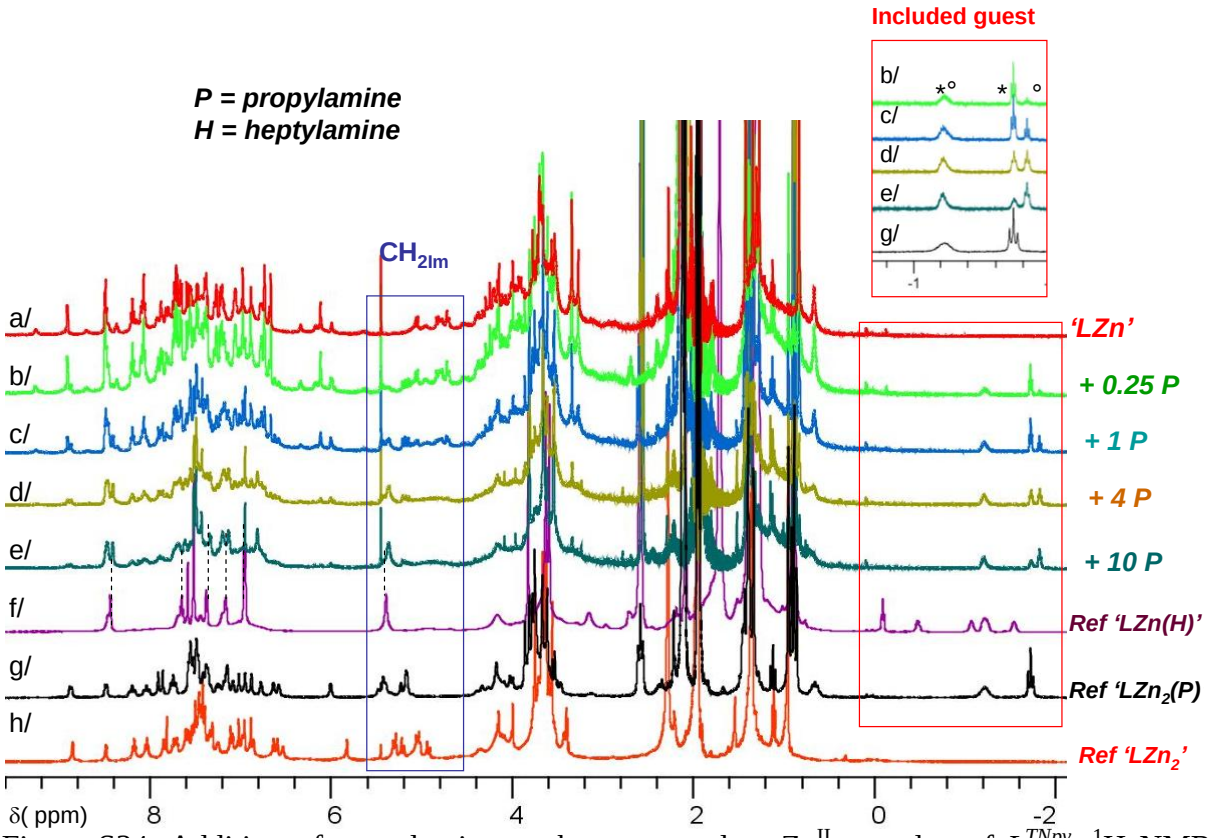


Figure S34. Addition of propylamine to the mononuclear $Zn^{II}$ complex of $L^{TNpy}$. $^1H$ NMR spectra ($CD_3CN$, 300K, 500 MHz) of a/ $L^{TNpy}$+ 1 eq $Zn^{II}$; b/ $L^{TNpy}$+ 1 eq $Zn^{II}$ + 0.25 eq propylamine; c/ $L^{TNpy}$+ 1 eq $Zn^{II}$ + 1 eq propylamine. d/ $L^{TNpy}$+ 1 eq $Zn^{II}$ + 4 eq propylamine. e/ $L^{TNpy}$+ 1 eq $Zn^{II}$ + 10 eq propylamine. f/ $L^{TNpy}$+ 1 eq $Zn^{II}$ + 10 eq heptylamine g/ $L^{TNpy}$+ 2 eq $Zn^{II}$ + 4 eq propylamine (250 MHz); h/ $L^{TNpy}$+ 2 eq $Zn^{II}$. * indicate the resonances of the included propylamine in $L^{TNpy}Zn_2$(propylamine)$^{4+}$, ° indicate the resonances of the included propylamine in $L^{TNpy}Zn$(propylamine)$^{2+}$. A mixture of mono- and dinuclear host-guest adducts are observed ([0,-2 ppm] window). For low guest concentrations (b/), the main adduct is the dinuclear one (reference spectrum: g/). For higher concentrations, the mononuclear adduct becomes predominant.

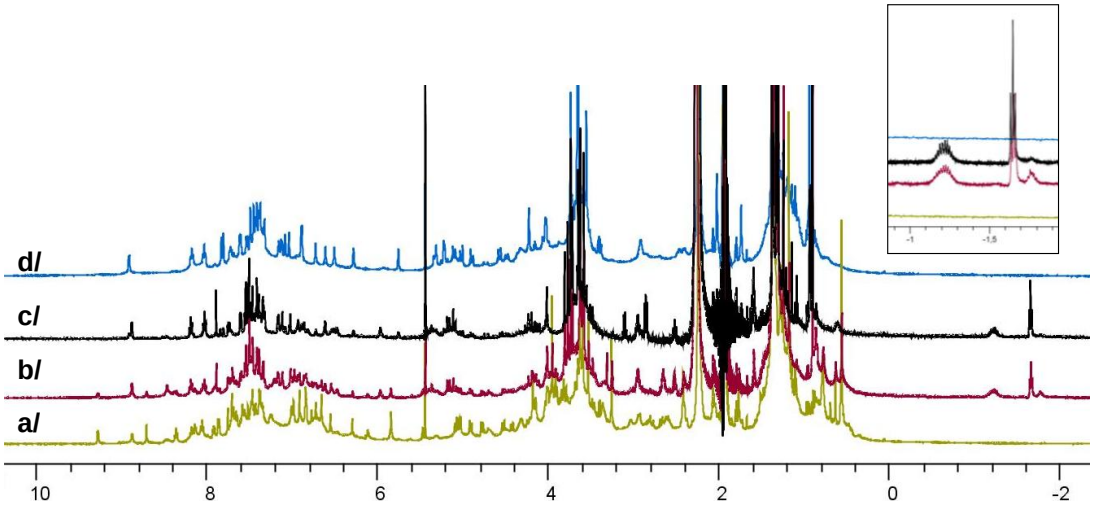


Figure S35. $^1H$ spectra ($CD_3CN$, 500 MHz, 275 K) of: a/ $L^{TNpy}_{C4NHBoc}$ +1 eq Zn ; b/ $L^{TNpy}_{C4NHBoc}$ +1 eq Zn + 2 eq propylamine ; c/ $L^{TNpy}_{C4NHBoc}$ +2 eq Zn + 2 eq propylamine ; d/ $L^{TNpy}_{C4NHBoc}$ +2 eq Zn.

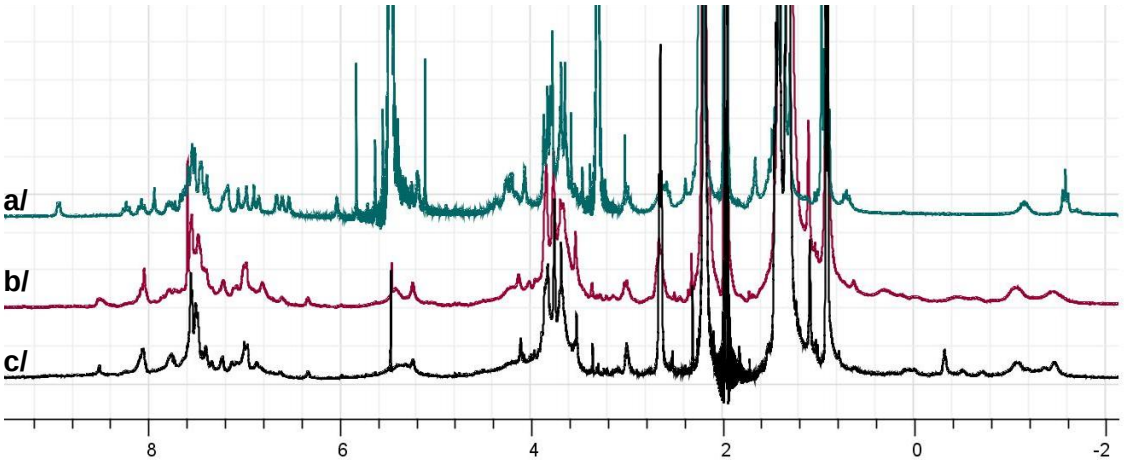


Figure S36. $^{1}$H spectra ($CD_3CN$, 300 K) of: a/ $L_{C4NHBoc}^{TNpy}$ +2 eq Zn + 4 equiv propylamine (250 MHz); b/ $L_{C4NHBoc}^{TNpy}$ +2 eq Zn + 4 equiv octadecylamine (250 MHz) ; c/ $L_{C4NHBoc}^{TNpy}$ +2 eq Zn + 4 equiv heptylamine (500 MHz).

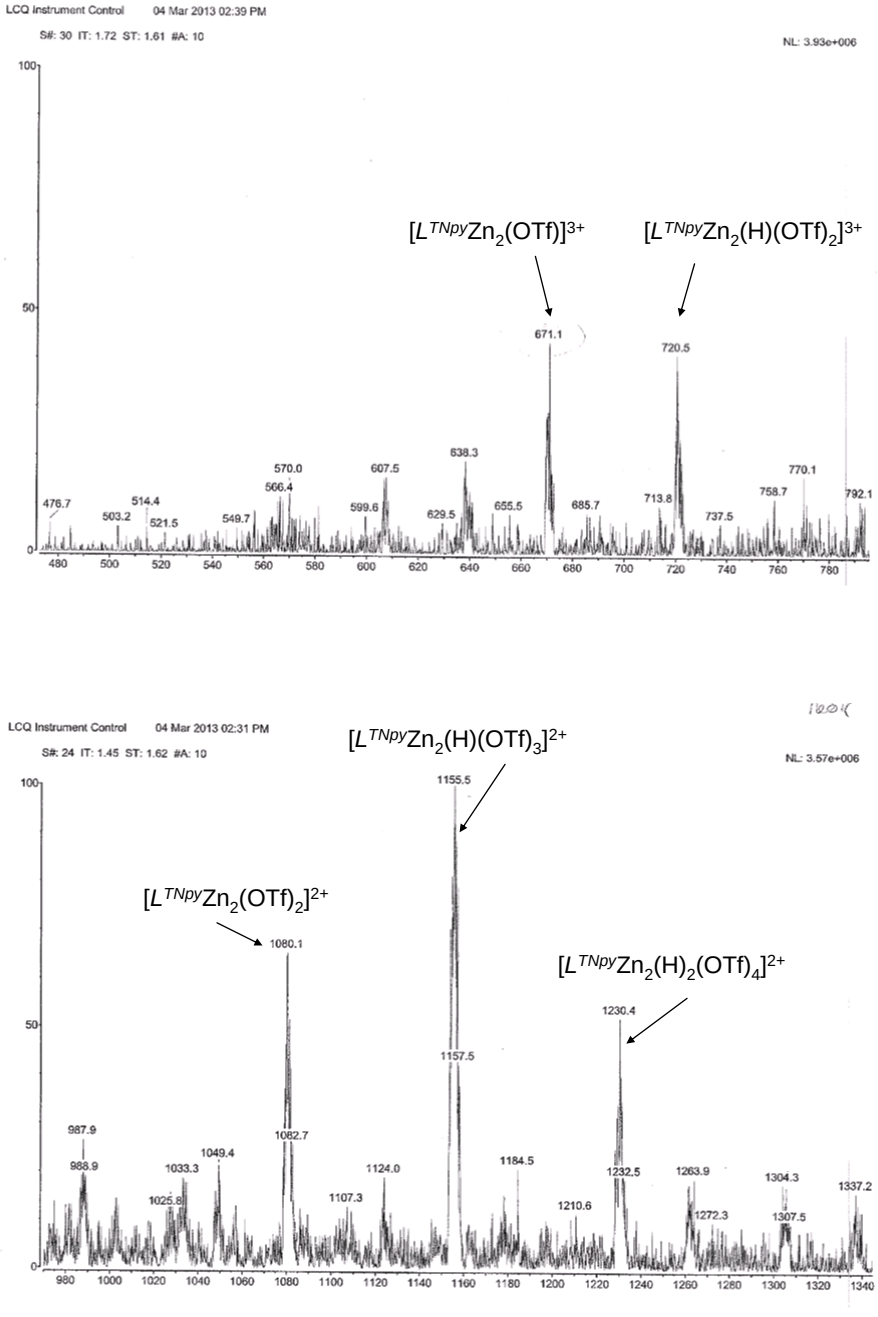


Figure S37. ESI-MS spectrum (postive mode) of a solution containing $L^{TNpy}$+ 4 eq $Zn(OTf)_2$ in $CH_3CN$ (injected in $CH_3OH$). $[L^{TNpy}Zn_2(OTf)]^{3+}$ : exp 671.1 [calcd 670.92 (100.0%), 670.59 (85.8%), 671.25 (82.5%)] ; $[L^{TNpy}Zn_2(H)(OTf)_2]^{3+}$ : exp 720.5 [calcd 720.91 (100.0%), 720.57 (86.5%), 721.24 (84.5%)] ; $[L^{TNpy}Zn_2(OTf)_2]^{2+}$: exp 1080.1 [calcd 1080.35 (100.0%), 1081.35 (95.8%), 1080.85 (90.9%)]; $[L^{TNpy}Zn_2(H)(OTf)_3]^{2+}$: exp 1155.5 [calcd 1155.33 (100.0%), 1156.33 (96.5%), 1155.83 (89.6%)]; $[L^{TNpy}Zn_2(H)_2(OTf)_4]^{2+}$: exp 1230.4 [calcd 1230.31 (100.0%), 1231.31 (98.5%), 1230.81 (89.0%)].